

9. PETROLOGICAL STUDIES ON DSDP LEG 34 BASALTS: NAZCA PLATE, EASTERN PACIFIC OCEAN¹

D.R.C. Kempe, Department of Mineralogy, British Museum (Natural History), London, England

ABSTRACT

Fourteen fairly to very fresh samples of oceanic basalt (generally LIL-element-depleted, MORB-type) from DSDP Sites 319, 320, and 321 have been examined. Site 319 basalt is an OL-tholeiite, falling in the olivine tholeiite field; texturally it ranges from glassy and variolitic to hyaloophitic, ophitic, and porphyritic. Phenocrysts, ranging up to 3 mm in diameter, are of granular pyroxene, plagioclase, and olivine largely, but not entirely, altered to smectite. Site 320 and 321 basalts extend over a finer grained textural range, with phenocrysts rarely exceeding 1 mm; Site 321 has some vesicles. Basalts from both sites are PL-tholeiites, falling in the quartz tholeiite field. Trace elements were determined and, in general, show normal behavior. Microprobe analyses are given of the pyroxene and plagioclase phenocrysts and groundmass phases; the former are all augites, those from Site 319 being more calcic than the others. Plagioclase forms large and small zoned phenocrysts, microphenocrystic laths, and groundmass laths; compositions range between An_{82} (phenocryst cores) and An_{46} (groundmass and phenocryst rims). Site 319 plagioclases show the greatest variation and include examples of reverse zoning. FeO is significantly present in the feldspar, inversely proportional to CaO. None of the basalts is very "primitive" (low FeO^*/MgO ratio) but basalt from Site 321 is highly fractionated, FETI-type basalt, remarkably similar to that from Site 256, Leg 26. The close juxtaposition of "primitive" (undifferentiated) or relatively "primitive" with FETI-type basalt, now found in two oceans, is discussed. Differentiation at Site 319 proceeds normally; plotted against depth, Fe/Mg and Ab/An enrichment occurs upwards. There is evidence of a second type of differentiation, possibly representing variation between successive waves of magma, rather than within each wave.

INTRODUCTION AND SCOPE OF PAPER

Fourteen basalt samples from the Nazca plate (eight from Site 319, two from Site 320, and four from Site 321) were examined in thin section and their bulk chemistry (major, minor, and some trace elements) determined. Electron microprobe analyses were made of phenocryst and groundmass phases (pyroxene and plagioclase) from six of the samples. Special attention was paid to the normative mineralogy and differentiation trends of the rocks; other aspects are described elsewhere in this volume. Leg 34 sites are the most southerly of those in the Pacific Ocean as well as the first from the Nazca plate, but three previous DSDP legs (5, 9, and 16) have operated nearby in the eastern margin of the Pacific Ocean, where samples were drilled from the Pacific plate.

The rocks from Site 319 are, along with those from Site 257 (from Leg 26), the freshest to be recovered by DSDP. Both reach a maximum sonic velocity (V_p) of

6.5 km/sec (Hyndman, 1974; Salisbury and Christensen, this volume).

PETROGRAPHY

Site 319

Basalt from Site 319 (Bauer Deep) is sometimes porphyritic and ranges in texture from glassy (Plate 1, Figure 1); variolitic (Plate 1, Figures 1 and 2; Plate 2, Figure 1); and hyaloophitic (Plate 1, Figure 5) to subophitic (Plate 1, Figure 4) and ophitic or diabasic (Plate 1, Figure 3). These textures, which are shown in the plates in order of increasing depth, represent variations in the cooling rate of parts of the five or even eight cooling units recognized; these units are considered more likely to be flows than pillow layers or sills. The textures displayed in these rocks are such that they cannot be described by simple textural terms; those used above are generalizations. However, the textural types reflect a cooling sequence in which the following stages, in which phenocrysts or microphenocrysts may or may not be present, are among the most important:

Glass (sideromelane) or palagonite if hydrated (sometimes vesicular), sometimes less rapidly quenched to become spherulitic or variolitic in which develop

¹With analytical contributions from J.C. Bevan, V.K. Din, and R.F. Symes.

plumose or sheaf-like varioles of pyroxene, forming in coarser grained varieties subophitic "islands" in residual glass patches (hyaloophitic) or else rocks that are totally subophitic or ophitic (diabasic), sometimes showing embayed plagioclase.

Bunch and LaBorde (this volume) give a full account of all aspects of the petrography of the rocks, and consequently only a summary is given here (Table 1). The rocks studied show a similar range of textures to those collected from a sequence of similar length from Site 257, Leg 26, southern Indian Ocean (Kempe, 1974). The Leg 34 rocks contain fewer large phenocrysts than those of Leg 26 but they are more widely distributed. There are far fewer vesicles and none is filled with the glauconitic mineral, celadonite, although a few grains of this mineral are present in Sample 2-1, 111-114 cm. Apart from Leg 26, celadonite is recorded from Leg 17 (Bass et al., 1973). The rather "runic" texture of Sample 3-1, 78-81 cm is interesting (Plate 1, Figure 3). The plagioclase laths are embayed against apparently earlier formed pyroxene grains, a texture very similar to that noted in one or two of the Leg 26 basalts and elsewhere (Kempe, 1974). The large phenocrysts in Sample 7-1, 121-124 cm are notable in that fresh olivine patches remain in crystals largely altered to smectite—a feature rare in drilled basalts.

Site 320

The basalt from Site 320 is thought to occur as pillows or thin flows, forming at least 10 cooling units. Both samples examined are variolitic; the upper contains a few small plagioclase phenocrysts (Table 2). The most notable feature is the morphology of the small laths and microlites of plagioclase; these form stellate bunches, occasionally cruciform groups, and are frequently bifurcate at each end like blunt, double-ended tuning forks (Plate 2, Figure 2). Olivine (always as pseudomorphs) is rarely present in the upper sample and is apparently absent in the lower one.

Site 321

The sequence of four samples from Site 321, Core 14, thought to come from extrusive units, are all hyaloophitic to subophitic, and, unlike the first two series described, are quite highly vesicular (Table 2). Olivine is notably absent, although the upper three samples contain traces and patches of smectite probably formed from the alteration of olivine. Calcite most commonly fills the vesicles, but some are empty and others contain palagonite or smectite. The Section 3, 7-10 cm sample also contains calcite in patches of mesostasis. Plagioclase laths embayed around preformed granular pyroxene are again present (see Site 319) in Sections 1, 42-45 cm; 3, 7-10 cm; and 4, 7-10 cm: (Plate 2, Figures 5 and 6).

CHEMISTRY

Methods

The XRF method of Norrish and Hutton (1969) was used to determine Si, Ti, Al, Fe, K, and P. The concentrations of other major, minor, and trace elements (Mg,

Ca, Na, Mn, Be, Cr, Ni, Li, Cu, Co, Zn, V, Sr, Ba, and Rb) were determined by atomic absorption spectrophotometry on solutions prepared according to the method of Langmyhr and Paus (1968); calibration curves were obtained from measurements on international standard rocks and synthetic standards. Five trace elements (Nb, Zr, Y, Pb, and Ga) were estimated semiquantitatively by a spectrographic method requiring the visual comparison of the sample spectra with those of synthetic standards. The French and Adams (1972) method served for the determination of ferrous iron with the modification that potassium permanganate replaced ceric sulphate as titrant. H_2O^- was measured gravimetrically and H_2O^+ and CO_2 by means of a CHN elemental analyzer (V.K. Din).

Results

All 14 samples studied (eight from Site 319, two from Site 320, and four from Site 321) have been analyzed. The analyses of basalts from Site 319 (Bauer Deep) are reported in Table 3 and those from the eastern margin of the Nazca plate in Table 4. Most of the rocks are relatively fresh. Using the criteria of Miyashiro et al. (1969), established on dredged rocks, an unweathered abyssal tholeiite usually contains less than 2% Fe_2O_3 and 1.2% H_2O , and has an $\text{Fe}_2\text{O}_3/\text{FeO}$ ratio of less than 0.3. A few of the rocks satisfy the water requirement, but none is within the Fe_2O_3 or iron ratio limits. However, most DSDP basalts are more highly altered or weathered than those from Leg 34, and also those from Leg 26 which are very similar in this context; basalts from Site 257 meet the Fe_2O_3 limitation but contain more H_2O^- (Kempe, 1974). Both holes (257 and 319) yielded sequences of comparable length and have maximum sonic velocities of 6.5 km/sec. As will be shown below, the Site 321 basalt bears a very close resemblance to that from Site 256 (Leg 26), with average Fe_2O_3 , FeO, and $\text{Fe}_2\text{O}_3/\text{FeO}$ values of 3.78 and 3.40, 9.83 and 9.87, and 0.38 and 0.34, respectively (Table 4).

Apart from the first two samples from Site 319 (319-13-1 and 319A-1-1), which differ from the remainder from this site in their low TiO_2 , FeO^* , and P_2O_5 and high MgO and CaO contents, the basalts from each site are fairly homogeneous, especially those from Site 321. Sample 320B-3-1 basalt is somewhat anomalous in its low SiO_2 and high Al_2O_3 , possibly through alteration, and the same applies, to a lesser extent, to the basalt from Sample 319A-5-1. By analogy with Site 256, homogeneity appears to be a characteristic of this type of Fe- and Ti-rich basalt. The SiO_2 content (Figure 1b) varies between 48.79% and 51.47% and all but four lie between 49% and 50%, thus falling very close to the average figure of 49.50% (Shido et al., 1971). All are low-alumina basalts, in that none has an Al_2O_3 content in excess of ca 16.4% (Miyashiro et al., 1969). In fact, only two have $\text{Al}_2\text{O}_3 > 15\%$, while Site 321 basalts, like those of Site 256, average ca 13%. With two or three exceptions, the $\text{Fe}_2\text{O}_3/\text{FeO}$ ratio is around 0.35 to 0.40, an average range for fresh DSDP basalts but higher than that for fresh dredged rocks. The total FeO^* values are typical, respectively, for "normal" oceanic basalt (the lower part of Site 319, 11.0%); fairly "primitive"

TABLE 1
Summary of Typical Characteristics of Basalt Samples From Site 319, Bauer Deep

Sample (Interval in cm)	Plate	Texture	Co-ordinates in olivine or quartz tholeiite field (from Table 3)	Olivine	Pyroxene	Plagioclase	Ore ^a
319-13-1, 77-80	1, Figure 1	Variolitic	$di_{70.6}hy_{28.4}ol_{1.0}$	Very rare, small, totally altered (?palagonite)	Plumose and granular	Laths up to 1 mm	Skeletal
319A-1-1, 48-51	—	Hyalophitic	$q_{0.3}di_{57.8}hy_{41.9}$	Patches of ?smectite may be altered olivine	Sheaf-like and plumose	Laths up to 1 mm	Skeletal
319A-2-1, 111-114	1, Figure 2	Coarse variolitic, some phenocrysts	$q_{7.2}di_{62.2}hy_{30.6}$	Possible patches of smectite after olivine	Sheaf-like and granular; phenocrysts: $Mg_{42}Fe_{17}Ca_{41}$ groundmass: $Mg_{43}Fe_{14}Ca_{43}$	Phenocrysts and laths up to 2 mm: An_{79-46} groundmass: An_{48}	Skeletal
319A-3-1, 78-81	1, Figure 3	Ophitic to very coarse hyalophitic, somewhat runic texture, some phenocrysts	$q_{3.4}di_{55.7}hy_{40.9}$		Long sheaves, up to 1.5 mm; phenocrysts: $Mg_{45-40}Fe_{13-21}$ Ca_{42-39} groundmass: $Mg_{46}Fe_{14}Ca_{40}$	Zoned phenocrysts up to 2 mm: An_{82-58} embayed laths over 2 mm long: An_{81-48} groundmass: An_{62-56}	Skeletal
319A-3-5 75-78	1, Figure 4	Subophitic, some phenocrysts	$q_{3.0}di_{52.0}hy_{45.0}$	Large smectites (2.5 mm) after	Granular	Few phenocrysts up to 3 mm	Granular
319A-5-1, 20-22	1, Figure 5	Hyalophitic, porphyritic	$q_{8.8}di_{67.3}hy_{23.9}$	Large smectites after olivine	Sheaf- and fan-like: $Mg_{45}Fe_{14}Ca_{41}$	Phenocrysts over 2 mm: An_{81-67} groundmass: An_{64}	Granular
319A-6-1, 93-98	1, Figure 6	Glassy (palagonitized)	$q_{5.7}di_{64.0}hy_{30.3}$	Small euhedral fresh and altered olivine	Rare grains	Rare phenocrysts up to 1 mm laths and "pins"	Granules in glass
319A-7-1, 121-124	2, Figure 1	Subvariolitic, porphyritic, rare vesicles	$q_{10.1}di_{57.5}hy_{32.4}$	Large phenocrysts (over 2 mm) partly but not entirely altered to smectite	Mostly granular, some sheaf-like, very small micro- phenocrysts; groundmass: $Mg_{40}Fe_{20}Ca_{40}$	Few small Phenocrysts (1 mm): An_{68} groundmass: An_{80-66}	Granules in glass

^aProbably mainly titanomagnetite (see Ade-Hall, this volume).

tholeiite (the upper part of Site 319, 8.8%, and Site 320, 8.5%); and fractionated, FETI-type (Fe- and Ti-rich) tholeiite (Site 321, 13.2%). The values for MnO and MgO are in no way remarkable; the Site 321 basalts, predictably, contain slightly higher MnO and lower MgO. In the case of CaO, only the very high values for the upper part of Site 319 are notable. The alkalis show no unusual features, falling well within the range for Na₂O of 2.5% to 3.1% and for K₂O of <0.3% (Shido et al., 1971). Two basalts from Site 319 have slightly higher K₂O than this, while those from Site 321 contain the least; none from Leg 34 has the exceptionally low K₂O content of basalts from Sites 14 and 18, Leg 3 (Frey et al., 1974) or even Site 257. TiO₂ and P₂O₅ values are unremarkable, both reaching their highest levels in Site 321 basalt and their lowest in the "primitive" upper part of Site 319.

Thus the Leg 34 basalts have major and minor element compositions typical of LIL-element (large-ion

lithophile)-depleted tholeiites, of MORB-type (mid-ocean ridge basalt) (Christensen et al., 1973). The Mg/(Mg + Fe) ratios of Sites 319 and 320 basalt (mean values, 0.54 and 0.59) are typical: that of Site 321 (0.45) indicates extreme fractionation, discussed in a later section. The low Cr and Ni (and Co and Cu) contents of Site 321 basalt, accompanied by high V (and Zn), correlate with this degree of fractionation, as at Site 256 (Figure 1). Similarly, low Al₂O₃ is accompanied by low CaO and thus by low Sr, although, surprisingly, Sr was not correlated with CaO and Al₂O₃ at Sites 256 and 257 (Kempe, 1974, Table 5). However, Sr is anomalous in that it is a typical LIL-element, depleted in "primitive" or primary MORB-type tholeiite, but also usually correlates with Al₂O₃, which is depleted by fractionation in FETI-type basalts at, for example, Sites 32 (Melson, 1973), 256, and 321 (but see Figure 2). Other elements less noticeably enriched with fractionation are Ga, Zr, and Y; this is illustrated by comparison of the values

TABLE 2
Summary of Typical Characteristics of Basalt Samples from Sites 320 and 321,
Eastern Margin of the Nazca Plate

Sample (Interval in cm)	Plate	Texture	Coordinates in Olivine or Quartz Tholeiite Field (from Table 4)	Olivine	Pyroxene	Plagioclase	Ore ^a
320B-3-1, 54-57	2, Figure 2	Variolitic, some phenocrysts	$q_{10.2}di_{62.9}hy_{26.9}$	Rare, altered (yellow) crystals	Granular: $Mg_{47-49}Fe_{13-19}$ Ca_{40-32}	Rare phenocrysts (1 mm); small laths; stellate, bifurcate, "tuning-fork": An_{73-63} groundmass: An_{70}	Granules in glass
320B-5, CC	2, Figure 3	Variolitic	$q_{5.3}di_{59.2}hy_{35.5}$	Absent	Sheaf-like and granular	Laths, about 0.5 mm	Skeletal
321-14-1, 42-45	2, Figure 4	Subophitic to hyaloophitic, vesicular (0.7 mm)	$q_{10.3}di_{47.0}hy_{42.7}$	Traces	Granular	Embayed laths, about 0.5 mm	Skeletal
321-14-2, 9-12	2, Figure 5	Hyaloophitic, vesicular	$q_{8.0}di_{57.3}hy_{34.7}$	Traces	Granular, clusters	Laths (up to 1 mm)	Skeletal
321-14-3, 7-10	—	Hyaloophitic, vesicular (calcite filled)	$q_{8.7}di_{44.4}hy_{46.9}$	Possible smectite pseudomorphs	Granular	Embayed laths; (up to 1 mm)	Coarse grains
321-14-4, 7-10	2, Figure 6	Subophitic to coarse hyalo- ophitic, rare vesicles	$q_{12.3}di_{41.3}hy_{46.4}$	Absent	Granular, clusters: $Mg_{46}Fe_{18}Ca_{46}$	Embayed laths phenocrysts (1.3 mm): An_{69-57} groundmass: An_{61}	Skeletal

^aProbably mainly titanomagnetite (see Ade-Hall, this volume).

from Site 257 with those from Site 256 and all Leg 34 sites. The low concentrations of the LIL-elements (Rb, Sr, Ba, Y, Zr) in the basalts from all three Leg 34 sites are generally typical of MORB basalt; other than the low strontium at Site 321, only the rather high Rb and Ba at Site 319 call for comment. Plotted on the Ti/100-Zr-Sr/2 diagram of Pearce and Cann (1973), all the Leg 34 basalts fall in the OFB (ocean-floor basalt) field.

In Table 5 some comparative average analyses are given. The Site 319 basalt most closely resembles the average of 13 analyses of Leg 16 basalts, also from the eastern Pacific Ocean (Yates et al., 1973 a, b), and that of 18 analyses from the Juan de Fuca and Gorda ridges (Kay et al., 1970). The Site 320 basalt resembles the average for 10 tholeiites from the East Pacific Rise and the Chile Rise (Hekinian, 1971), except that the Leg 34 rock has less iron. It also resembles the average oceanic tholeiite of Engel et al. (1965) except that it is low in Al_2O_3 . Finally, the Site 321 basalt average can only be compared with a similar rock such as that from Site 256, Leg 26. The ferrobasalts from the Mid-Atlantic Ridge are similar in iron content, but usually contain less SiO_2 and more Al_2O_3 (Bald Mountain, 45°N: Aumento and Loncarevic, 1969) or more CaO (53°N: Hekinian and Aumento, 1973). What is truly remarkable is the homogeneity of the DSDP FETI basalts (Sites 256, 321, and even 32) at and between each site. It may be that the average compositions for drilled basalts at varying

stages of fractionation and from different tectonic settings will prove to be significantly different from the compositional averages for dredged rocks.

Normative Mineralogy and Classification

The basalts have been plotted in the Yoder and Tilley (1962) projection Ne-Di-Ol-Hy-Q, normalized on a *cc*-free, $Fe_2O_3 = 1.50\%$ basis (Table 6 and Figure 3). The Site 319 basalt is an olivine tholeiite, the average containing 10% *ol*. One analysis of the Site 320 basalt contains *ol*, but the other sample and the average for this site, unlike the "primitive" upper part of the Site 319 basalt, as well as the Site 321 basalt, all plot in the *q-di-hy* field. The pair 320 and 321 thus resemble in some respects the pair 256 and 257 from Leg 26; both pairs represent "primitive" (257) or relatively "primitive" (320), and highly fractionated quartz tholeiites closely juxtaposed within the same geomorphological feature. They provide further evidence that there is a strong tendency for drilled basalt to be less olivine normative or even distinctly quartz normative when compared with dredged basalt (Kempe, 1974; 1975).

Although these are low-alumina basalts in the sense of Miyashiro et al. (1969), all of the Leg 34 rocks plot in the high Al_2O_3 field in the alkalis ($Na_2O + K_2O$) versus SiO_2 diagram of Kuno (1960). Basalt from Site 319 is an OL-tholeiite (Miyashiro et al., 1970; Shido et al., 1971), as would be expected from its modal and normative com-

TABLE 3
Chemical Analysis of Olivine Tholeiites From Site 319, Bauer Deep^a

	Sample (Interval in cm)							
	319-13-1, 78-80	319A-1-1, 48-51	319A-2-1, 111-114	319A-3-1, 78-81	319A-3-5, 75-78	319A-5-1, 20-22	319A-6-1, 93-98	319A-7-1, 121-124
SiO ₂	50.56	50.15	49.44	49.89	49.60	48.79	49.54	49.52
TiO ₂	1.22	1.20	2.01	2.11	2.00	2.00	1.90	1.83
Al ₂ O ₃	15.38	14.78	14.09	14.34	14.42	14.44	14.41	14.29
Fe ₂ O ₃	2.55	2.59	5.07	3.10	2.94	6.33	4.24	5.20
FeO	5.79	7.32	6.92	8.27	8.34	5.23	6.76	5.96
MnO	0.17	0.17	0.18	0.17	0.17	0.20	0.18	0.18
MgO	7.41	7.95	6.51	6.67	6.97	6.55	6.56	7.09
CaO	13.35	12.29	11.04	11.03	10.90	11.16	11.49	11.15
Na ₂ O	2.74	2.51	2.93	2.95	2.81	3.04	2.75	2.71
K ₂ O	0.11	0.05	0.25	0.12	0.11	0.32	0.35	0.18
H ₂ O ⁺	0.43	0.59	0.66	0.65	0.66	1.19	0.70	0.88
H ₂ O ⁻	0.56	0.55	0.93	0.70	0.74	1.06	0.85	0.75
P ₂ O ₅	0.08	0.08	0.18	0.20	0.17	0.16	0.17	0.17
CO ₂	0.24	0.23	0.18	0.25	0.27	0.33	0.10	0.27
Total	100.59	100.46	100.39	100.45	100.10	100.80	100.00	100.18
Trace Elements (ppm)								
Ti	7,314	7,194	12,050	12,649	11,990	11,990	11,391	10,971
Be	<1	1	1	1	2	2	1	1
Ga	40	40	50	50	50	50	50	50
Cr	255	255	230	230	235	225	245	240
Li	9	7	9	13	11	30	8	8
Nb	<50	<50	<50	<50	<50	<50	<50	<50
Ni	50	115	70	50	60	100	100	50
Co	85	85	100	90	95	65	70	65
Cu	95	15	30	15	15	70	65	25
V	335	310	355	355	325	390	375	325
Zn	70	80	85	90	85	80	80	80
Zr	120	150	200	200	200	200	200	200
Y	25	25	50	50	50	50	75	75
Sr	115	100	115	115	115	135	115	105
Ba	40	50	40	30	<30	<30	<30	<30
Rb	<5	<5	9	<5	<5	7	5	<5
Pb	<5	<5	<5	<5	<5	n.d. ^b	n.d. ^b	<5
Norms								
<i>q</i>	—	0.13	2.58	1.31	1.16	2.82	2.11	3.68
<i>or</i>	0.65	0.30	1.48	0.71	0.65	1.89	2.07	1.06
<i>ab</i>	23.18	21.24	24.79	24.96	23.78	25.72	23.27	22.93
<i>an</i>	29.35	28.92	24.56	25.54	26.41	24.82	25.95	26.30
<i>di</i>	27.99	24.34	22.37	21.37	20.19	21.54	23.56	20.83
<i>hy</i>	11.28	17.66	11.03	15.68	17.44	7.66	11.13	11.73
<i>ol</i>	0.40	—	—	—	—	—	—	—
<i>mt</i>	3.70	3.75	7.35	4.49	4.26	9.18	6.15	7.54
<i>il</i>	2.32	2.28	3.82	4.01	3.80	3.80	3.61	3.48
<i>ap</i>	0.19	0.19	0.42	0.47	0.40	0.38	0.40	0.40
<i>cc</i>	0.55	0.52	0.41	0.57	0.61	0.75	0.23	0.61
FeO*/MgO	1.09	1.21	1.76	1.66	1.58	1.67	1.61	1.50

^aAnalyst: V.K. Din.

^bn.d. = not detected.

TABLE 4
Chemical Analyses of Quartz Tholeiites From the Eastern
Margin of the Nazca Plate^a

	Sample (Interval in cm)					
	320B-3-1, 54-57	320B-5, CC	321-14-1, 42-45	321-14-2, 9-12	321-14-3, 7-10	321-14-4, 7-10
SiO ₂	49.47	51.47	49.69	49.20	49.16	49.87
TiO ₂	1.54	1.85	2.43	2.39	2.42	2.40
Al ₂ O ₃	16.10	14.83	13.14	12.96	13.08	13.18
Fe ₂ O ₃	4.41	2.49	3.88	3.60	3.83	3.81
FeO	4.53	6.26	10.11	9.58	9.71	9.90
MnO	0.14	0.18	0.23	0.22	0.18	0.18
MgO	6.21	7.37	6.20	6.12	6.43	6.20
CaO	11.78	11.64	10.19	11.19	9.66	9.57
Na ₂ O	2.82	2.85	2.54	2.52	2.76	2.64
K ₂ O	0.22	0.23	0.14	0.11	0.16	0.12
H ₂ O ⁺	1.45	0.69	0.59	0.67	0.87	1.10
H ₂ O ⁻	1.39	0.45	0.47	0.58	1.25	1.12
P ₂ O ₅	0.14	0.19	0.24	0.25	0.25	0.23
CO ₂	0.28	0.10	0.19	1.29	0.33	0.30
Total	100.48	100.60	100.04	100.68	100.09	100.62
Trace Elements (ppm)						
Ti	9,232	11,091	14,568	14,328	14,508	14,388
Be	1	1	1	<1	1	1
Ga	50	40	50	50	50	50
Cr	330	220	130	125	125	130
Li	40	11	9	14	13	11
Nb	<50	<50	<50	<50	100	<50
Ni	150	90	50	40	40	50
Co	75	80	65	60	65	60
Cu	80	75	30	20	15	30
V	310	325	470	460	420	455
Zn	70	90	110	110	110	105
Zr	150	200	200	200	200	200
Y	75	75	60	50	50	50
Sr	125	140	90	100	90	90
Ba	30	<30	<30	30	<30	<30
Rb	<5	<5	<5	<5	<5	<5
Pb	n.d. ^b	<5	<5	n.d. ^b	n.d. ^b	<5
Norms						
q	3.22	2.07	4.26	4.95	3.42	4.97
or	1.30	1.36	0.83	0.65	0.95	0.71
ab	23.86	24.11	21.49	21.32	23.35	22.34
an	30.63	27.00	24.04	23.73	22.83	23.76
di	19.86	23.19	19.47	18.01	17.47	16.64
hy	8.49	13.94	17.66	17.49	18.47	18.68
ol	-	-	-	-	-	-
mt	6.39	3.61	5.63	5.22	5.55	5.52
il	2.92	3.51	4.61	4.54	4.60	4.56
ap	0.33	0.45	0.57	0.59	0.59	0.54
cc	0.64	0.23	0.43	-2.93	0.75	0.68
FeO*/MgO	1.37	1.15	2.19	2.09	2.05	2.15

^aAnalyst: V.K. Din.^bn.d. not detected.

positions (Tables 1, 3, and 6), although two analyses plot on the boundary (cotectic) curve; the Site 320 and 321 basalts plot as PL-tholeiites (Figure 4), even though fresh olivine was found in other samples from both these holes, as are those from Sites 257 and 256. When fresh, all the basalts from Sites 319, 320, and 321 plot as pyroxene-tholeiites in the system of Hekinian and Aumento (1973), although when altered they may fall within the plagioclase-tholeiite field (Figure 5). Again, the Site 321 basalts plot in positions almost identical to those from Site 256.

It is interesting to compare the Leg 34 basalts with those from Leg 26. Those from Sites 321 and 256 are virtually identical. The Site 320 basalt seems to be intermediate between the Site 256 and 257 basalts in some respects, but in others lies between 257 and 251, the latter being a typical and very fresh spreading ridge quartz tholeiite from the Southwest Branch of the Mid-Indian Ocean Ridge. Most interesting of all, Site 319 basalt, a slightly undersaturated olivine tholeiite, very closely resembles the Site 251 quartz tholeiite in almost all chemical respects, but bears no resemblance at all to the very mildly alkaline, strongly undersaturated olivine tholeiite from Site 250, in the Mozambique Basin (Kempe, 1974), which is probably of the transitional LIL-element- and REE-enriched (rare-earth element) type of DSDP olivine tholeiite (Christensen et al., 1973). The Site 319 basalt thus has no clear analogy among the Leg 26 rocks, nor does the Site 250 basalt in Leg 34. Comparisons with Leg 16 basalts indicate that the average for those basalts is a PL-tholeiite close to the Site 320 basalt (Figure 4), and a pyroxene-tholeiite falling within the Site 319-320 cluster (Figure 5); it is very similar indeed to the Site 251 basalt from the Indian Ocean.

Crystallization Differentiation

The Leg 34 basalts have been plotted in several ways to show their degree of fractionation in comparison with basalts from other sites. In Figure 6a, the FMA diagram shows the basalts from the three sites to have a slightly more restricted range than those from Leg 26. Site 321 basalts again fall in an identical position to those from Site 256, and the Site 319 and 320 basalts fall between this point and the average for Site 257. The average for the Leg 16 basalts (Yeats et al., 1973a,b) lies within the Site 319 cluster. Similarly, the inset Figure 6b shows a tight cluster in the lime-alkalis diagram, with the Leg 16 average falling within it.

The two parameters, Mg/Fe* and Ab/An, are combined in Figure 7 in a fractionation diagram. The main group of Site 319 basalts, covering up to eight cooling units, shows a clear trend practically along the generalized direction. Trends for Sites 163 (eastern Pacific Ocean), 146 (Caribbean Sea), and 256 and 257 (Wharton Basin, southern Indian Ocean) are also shown. If these trends are shown plotted against depth below sediment-basalt contact (Figures 8,9, and 10), and assuming that all the basalts (except at Site 146) are flows and not sills, some interesting features emerge. Sites 319, 163, and 146 show "normal" trends, with enrichment in iron and alkalis upwards, while Sites 256 and 257—a series of

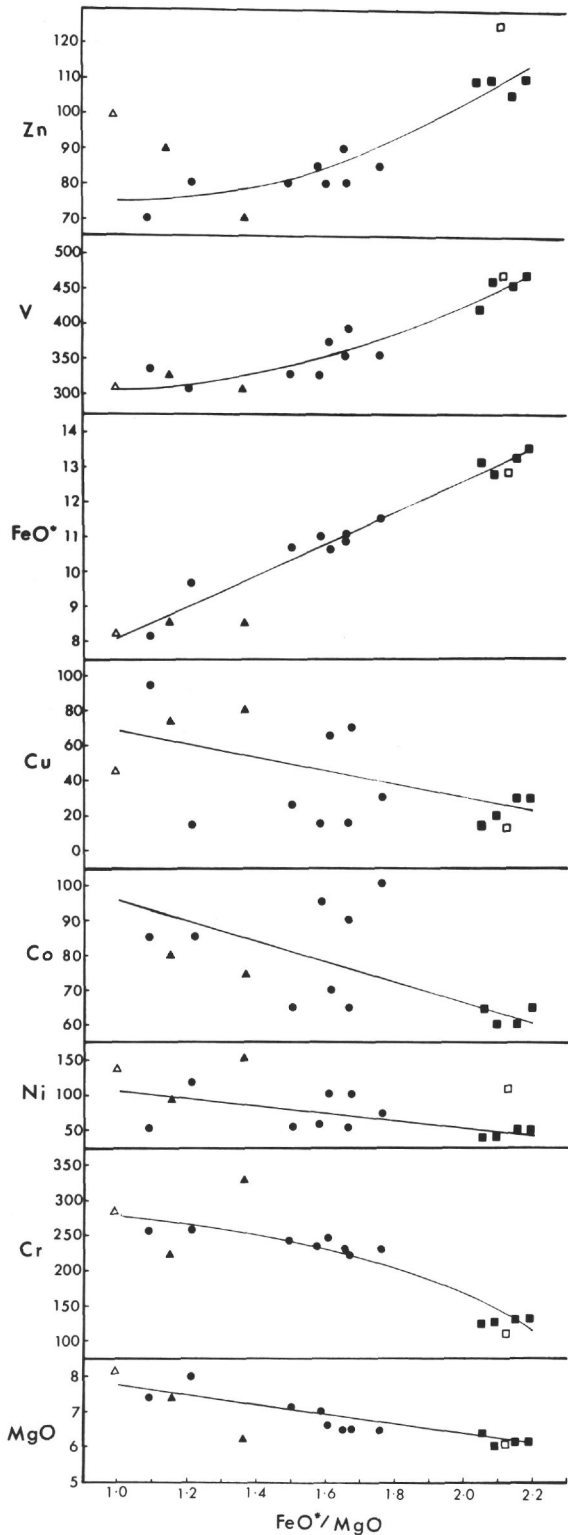


Figure 1a. Major and minor (wt%) and trace (ppm) elements plotted against FeO^*/MgO ratio for the Leg 34 basalts. Transition and other elements tending to increase or decrease with Fe/Mg variation.

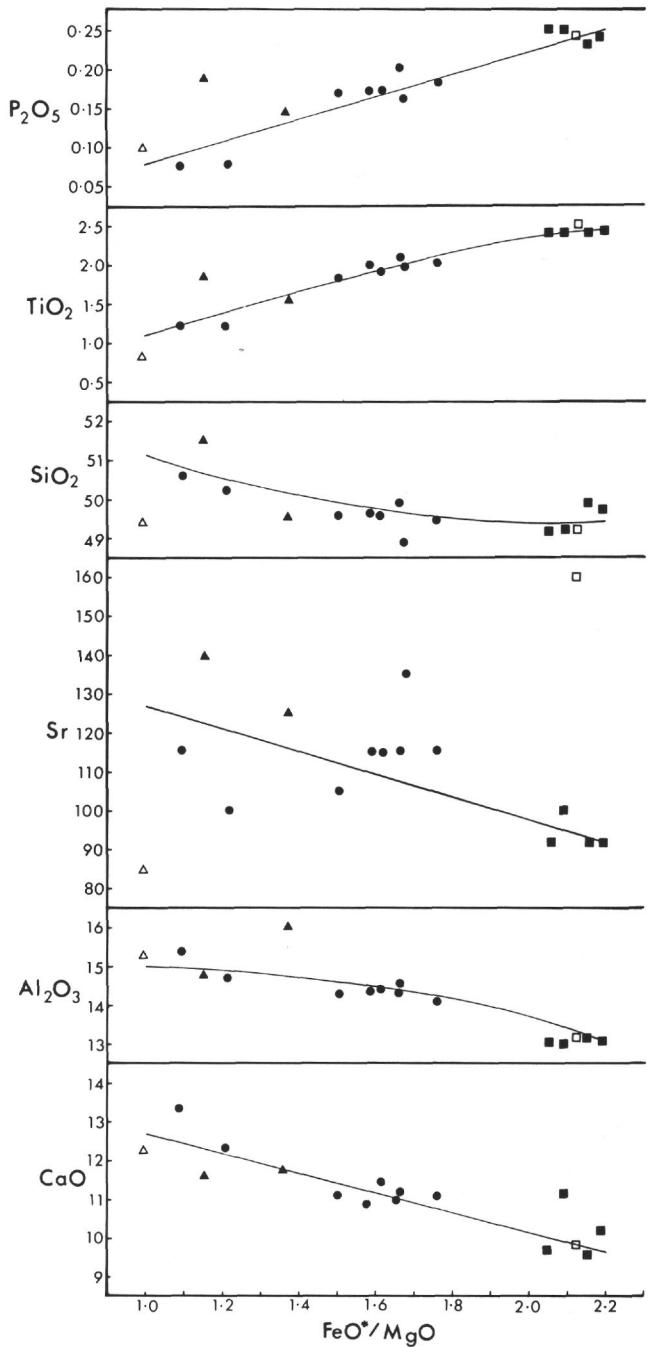


Figure 1b. TiO_2 and P_2O_5 ; Al_2O_3 , CaO and Sr ; and SiO_2 . Symbols as follows: ● Site 319; ▲ Site 320; ■ Site 321; △ Site 257 ("primitive"); □ Site 256 (FETI-type). The latter two symbols = average compositions of the basalts from the southern Wharton Basin, southeastern Indian Ocean (Kempe, 1974).

seven or eight or more flows—are, in different ways, anomalous (Kempe, 1974; 1975). However, the points at

Site 163, although thought on the evidence of the glassy selvages to represent seven flow units (Yeats et al., 1973a,b), are in effect only two, separated by a recovery gap (void), while those at Site 146 are an intrusive dolerite sill (Donnelly et al., 1973). At Site 319, the two uppermost samples (319-13-1 and 319A-1-1), which have been approximately equated allowing for the 13

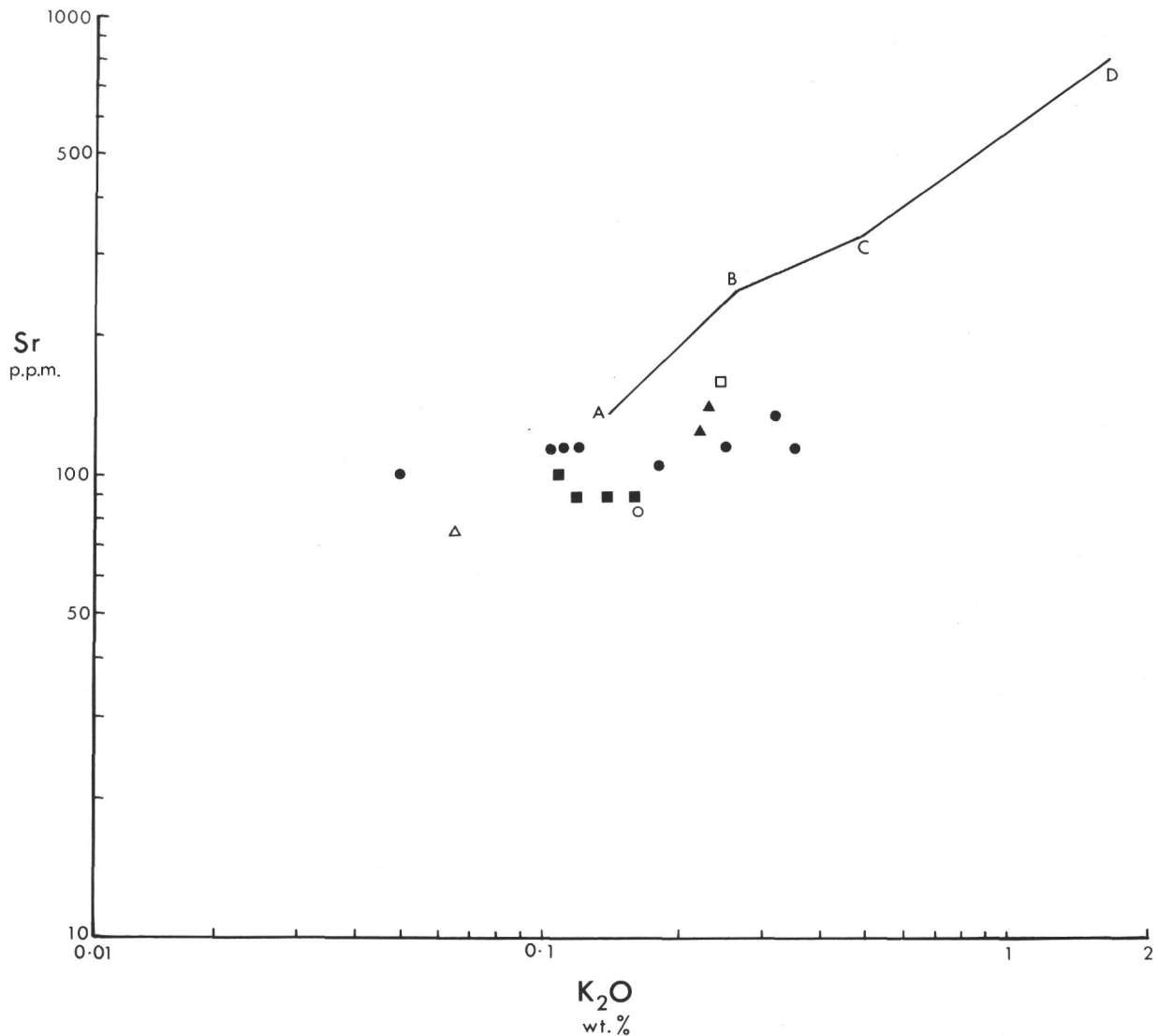


Figure 2. K_2O versus Sr (log-log) plot for the Leg 34 basalts (after Hart et al., 1970). (A) ocean floor basalt; (B) low-K tholeiite; (C) tholeiite; (D) alkali basalt (Hart et al., 1970, Table 2). Symbols as in Figure 1 except for open triangle (average fresh Site 257 basalts) and open circle (average of all Site 257 basalts).

meters difference in depth of the contact, show totally different values from those of the remaining six, as suggested by their bulk chemistry (Table 3). This change is also noted by Thompson et al. (this volume), who find an increase in the lower units in the concentrations of such elements as V, Y, Zr, Sr, and REE, and a decrease in Ni, Co, and Cr. The six points, however, show a practically linear trend for both FeO^* and CaO, the only anomalous point, for CaO, being the most altered rock (319A-5-1). Possibly this linear differentiation represents fractionation within flows (? one or more cooling units) whereas the more sudden change reflects major differentiation, in the opposite direction, within the magma chamber from which each flow derives. Until a core extending several hundred meters into layer 2 (?Leg 37) has been recovered, the true nature of fractionation upwards, discussed by Kempe (1975) cannot be determined. Figures 9 and 10 show the Site 319 curves alongside the ranges for Sites 32, 320, and 321,

the cores from which are too short to be plotted against depth, and the trends for Sites 163, 146, 256, and 257. These represent all the drilled basalt sequences which can be plotted against depth for which analyses are available; as stated above, the problem will not be solved until a long core (ca 500 m) is available. The Site 319 basalts show the clearest evidence of olivine phenocryst precipitation as a mechanism of fractionation, being the most convincing example of an OL-tholeiite among the long cores studied (see Figure 4). Most of the remainder, especially that from Site 257, plot as PL-tholeiites, lying in the quartz tholeiite field, in which most of the olivine phenocrysts have been destroyed by resorption and alteration.

The anomalous differentiation patterns in basalts from Sites 256 and 257 may perhaps be explained as part of the "rippling" or stepped curve if FeO^* or CaO are plotted against depth for a long core. Possibly each flow, cooling unit, or even pillow, can show its own differen-

TABLE 5
Some Comparative Average Basalt Compositions

	Leg 34 (Average of 14 Analyses)	Site 319 (Average of 8 Analyses)	Site 320 (Average of 2 Analyses)	Site 321 (Average of 4 Analyses)	Leg 5 ^a (Site 32- 14-1)	Leg 16 ^b (Average of 13 Analyses)	Legs 5 & 9 ^c (Average of 7 Analyses)	East Pacific ^d (Average of 18 Analyses)	East Pacific ^e (Average of 10 Analyses)	Oceanic ^f tholeiite (Average)	Site 256 ^g (Average of 3 Analyses)	Site 257 ^h (Average of 12 Analyses)
SiO ₂	49.74	49.69	50.47	49.48	51.91	49.67	50.62	50.50	49.96	49.94	49.20	49.38
TiO ₂	1.95	1.78	1.70	2.41	3.14	1.66	1.53	1.80	1.69	1.51	2.51	0.91
Al ₂ O ₃	14.25	14.52	15.47	13.09	12.58	14.50	15.75	15.30	15.52	17.25	13.18	15.26
Fe ₂ O ₃	3.86	4.00	3.45	3.78	—	—	—	—	2.14	2.01	3.40	2.32
FeO	7.48	6.82	5.40	9.83	15.30 ⁱ	10.30 ⁱ	9.35 ⁱ	11.00 ⁱ	8.33	6.90	9.87	6.08
MnO	0.18	0.18	0.16	0.20	[0.18]	[0.18]	[0.18]	[0.18]	0.18	0.17	0.19	0.19
MgO	6.73	6.96	6.79	6.24	5.04	7.12	7.67	7.00	7.25	7.28	6.10	8.25
CaO	11.17	11.55	11.71	10.15	8.98	10.53	11.45	11.20	11.01	11.86	9.92	12.25
Na ₂ O	2.76	2.81	2.84	2.62	2.62	2.72	2.67	2.70	2.73	2.76	2.67	2.09
K ₂ O	0.18	0.19	0.22	0.13	0.17	0.32	0.37	0.18	0.21	0.16	0.24	0.16
H ₂ O ⁺	0.80	0.72	1.07	0.81	—	1.15	—	—	0.73	—	0.72	0.75
H ₂ O ⁻	0.82	0.77	0.92	0.86	—	0.98	—	—	—	—	1.28	1.69
P ₂ O ₅	0.18	0.15	0.17	0.24	0.31	[0.15]	0.23	[0.15]	0.21	0.16	0.24	0.10
CO ₂	0.23	0.23	0.19	0.24	—	—	—	—	—	—	0.55	0.63
Total	100.33	100.37	100.56	100.08	100.23	99.28	99.82	100.01	99.96	100.00	100.07	100.06

^aDrilled FETI-type basalt, eastern Pacific Ocean (Melson, 1973).

^bDrilled basalts from the eastern Pacific Ocean (Yeats et al., 1973a, b).

^cDrilled basalts from the eastern Pacific Ocean (Melson, 1973).

^dDredged basalts from the Juan de Fuca and Gorda ridges, eastern Pacific Ocean (Kay et al., 1970).

^eDredged basalts from the East Pacific Rise and the Chile Rise (Hekinian, 1971).

^fAverage oceanic tholeiite (Atlantic and Pacific oceans) (Engel et al., 1965).

^{g,h}Drilled FETI and "primitive" basalts from the southern Wharton Basin, Southeastern Indian Ocean (Kempe, 1974).

ⁱTotal iron as FeO*.

TABLE 6
Normative Compositions on a cc-free, $Fe_2O_3 = 1.50\%$,
Basis, Recalculated to 100%

Sample (Interval in cm)	q	di	hy	ol
319-13-1, 77-80	—	71.17	18.21	10.62
319A-1-1, 48-51	—	58.55	32.83	8.62
319A-2-1, 111-114	—	58.32	30.26	11.42
319A-3-1, 78-81	—	56.09	38.30	5.61
319A-3-5, 75-78	—	53.04	41.42	5.54
319A-5-1, 20-22	—	62.25	16.03	21.72
319A-6-1, 93-98	—	60.53	31.90	7.57
319A-7-1, 121-124	—	55.01	39.31	5.68
320B-3-1, 54-57	—	61.13	35.54	3.33
320B-5, CC	2.00	58.76	39.24	—
321-14-1, 42-45	2.93	46.23	50.84	—
321-14-2, 9-12	1.82	55.65	42.53	—
321-14-3, 7-10	0.79	45.29	53.92	—
321-14-4, 7-10	4.45	42.12	53.43	—

tiation pattern, although this seems unlikely at both Sites 257 and 319, in each of which seven or more “flow units” are recognized. This concept could, of course,

apply to each “flow” in a magmatic sense, rather than that in which “flows” are recognized in a drill core. In effect it would mean each effusion or burst of magma, perhaps produced by the melting of different mantle fractions and capable of producing a total thickness of lava of some 300 meters, sometimes differentiated to the maximum possible extent (Kempe, 1975). The remarkable association of “primitive” or relatively “primitive” basalt with highly fractionated rock, which occurs at Sites 256 and 257 in the Wharton Basin, and again at Sites 320 and 321 near the eastern margin of the Nazca plate, is again noted in case it relates to the differentiation patterns. Unfortunately, the Leg 34 cores are, as already stated, too short to be plotted against depth.

PHASE CHEMISTRY

Electron microprobe analyses were made of pyroxene and plagioclase feldspars from suitable sections from the three holes studied. Where possible, phenocrysts of varying type, including core and rim portions of zoned crystals, and groundmass minerals, were analyzed in

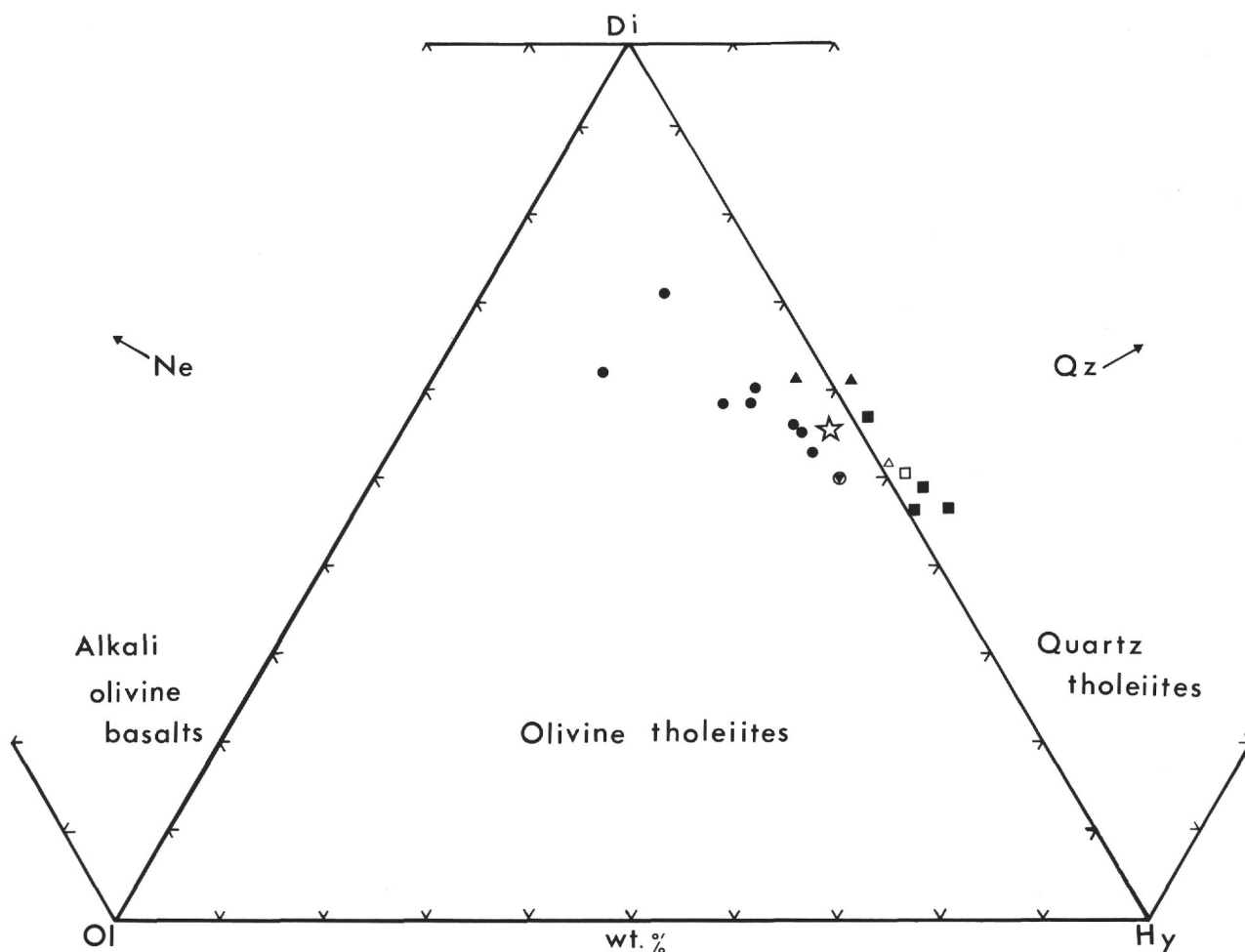


Figure 3. Normative compositions of the Leg 34 basalts, normalized on a cc-free, $Fe_2O_3 = 1.50\%$, basis (Table 6), plotted in the Yoder and Tilley (1962) projection. Site 319 basalts are olivine tholeiites, Sites 320 and 321 are quartz tholeiites. Symbols as in Figure 1, with open star, average for Leg 34; and triangle-within-circle, average for Leg 16 basalts (Yeats et al., 1973a, b).

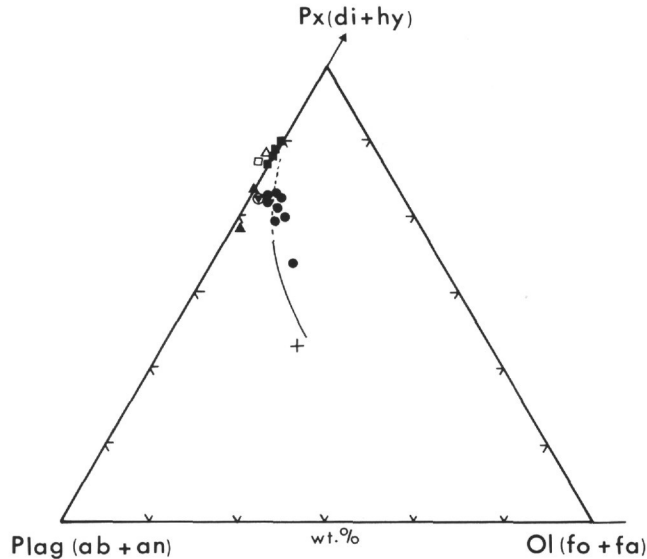


Figure 4. Leg 34 basalts plotted in the normative (normalized) diagram $Px(di + hy) - Ol(fo + fa) - Pl(ab + an)$. The full line represents a cotectic curve (Miyashiro et al., 1970). Symbols as in Figure 1, with triangle-within-circle, average for Leg 16 basalts; cross, Site 250 basalt (Kempe, 1974).

each rock. The results are reported in Tables 7 to 14, in which individual and average analyses are given to show typical compositions and compositional ranges. All analyses are plotted in Figures 11 and 12. Although relict olivine is present as large phenocrysts in basalts from Sample 319A-7-1, 121-124 cm and as small fresh crystals in Sample 319A-6-1, 93-98 cm, crystals suitable for analysis were not found in the probe sections. The interstitial glass and its alteration products, and ore minerals, were not studied.

The analyses were made on a Cambridge Instruments Geoscan at an accelerating voltage of 15 kv and a specimen current of about $0.6 \times 10^{-7} \text{A}$. Independently analyzed minerals of appropriate composition were used as standards, except for Cr and Mn when pure metals were used. A secondary augite standard was run with all analyses as a check of precision and accuracy. Results were corrected after the method outlined by Sweatman and Long (1969), using the BM-IC-NPL computer program (Mason et al., 1969). The pyroxene analyses were checked for correct stoichiometric proportions (R.F. Symes and J.C. Bevan).

Pyroxenes

All the pyroxenes analyzed are augites (Figure 11; Tables 7 and 8); no pyroxenes of salitic or endiopsidic composition, found in some drilled basalts, were encountered.

Table 7 and Figure 11 show the relatively slight variation between the compositions of phenocryst and groundmass pyroxenes; one of the largest ranges (8% Fs) is between core and rim in a phenocryst from Sample 319A-3-1, 78-81 cm. This section is perhaps the most interesting of those analyzed. Whereas the general tendency is for groundmass pyroxenes to be enriched in iron

relative to magnesium when compared with phenocryst pyroxenes, owing to normal fractionation, those in 319A-3-1 have the opposite trend, although the variation is small. Core and rim variation, on the other hand, follows the expected outward iron enrichment. This rock has an unusual "runic" texture (Plate 1, Figure 3), consisting of intergrown groundmass pyroxene and plagioclase. It is possible that late and rapid quenching, possibly due to pressure changes, resulted in the intergrowth and the Mg-rich nature of the pyroxene. Although zoned, Site 319A pyroxenes do not appear to show "compositional domains" as found in Leg 16 basalts (Yeats et al., 1973a,b). Sample 319A-5-1, 20-22 cm shows some exsolution of a Ca-poor pyroxene.

The augitic pyroxenes in basalts from Hole 320B and Site 321 are slightly less calcic than those from Hole 319A (Figure 11). As indicated by the bulk chemistry of the rock, Hole 320B basalt is, with the upper Hole 319 basalt, the most "primitive" of the Leg 34 rocks, with pyroxene lying close to the endiopsidic boundary, while augites in basalt from Site 321, as might be expected, resemble those from Site 256, Southeast Indian Ocean (Kempe, 1974).

The minor element chemistry shows that the pyroxenes contain typically small amounts of MnO (Yeats et al., 1973a,b) and, where determined, Cr_2O_3 . Alumina is high in Site 320B basalt, and variable but high in samples from Site 319A. The Site 321 pyroxenes, as might be expected from a FETI-type rock, contain low amounts of Al_2O_3 , as do those from the similar rocks from Site 256. This bulk composition characteristic is not reflected in the pyroxenes in the case of TiO_2 , however. Despite the high amounts of this oxide in rocks from Sites 256 and 321, the pyroxenes are notably low in TiO_2 , which presumably follows the (high) iron to form Fe-Ti oxides. In pyroxenes from Sites 319 and 320, TiO_2 occurs at a generally 1.5% to 2% level; it is notably low in those from 319A-3-1, where, as already mentioned, the bulk of the groundmass pyroxene is iron poor.

Plagioclase Feldspars

The plagioclase phenocrysts and groundmass laths show a fairly considerable range in composition (Figure 12, Tables 9 to 14). Basalts from Site 319A show the widest limits: Section 2-1 has An_{46-78} , and 3-1 An_{48-82} , with one zoned phenocryst extending to An_{42} . The most common range is An_{60-70} , a compositional range occupied by feldspars in typical spreading-ridge basalt such as that from Site 251, Southwest Branch of the Mid-Indian Ocean Ridge. Site 321 plagioclase is also typically An_{60-70} , surprisingly calcic when compared with plagioclase in the range An_{50-60} from the otherwise similar FETI basalt from Site 256 (Kempe, 1974).

Phenocrysts are scarce in basalts from Hole 320B and Site 321 and in those from the lower sections of Hole 319A. In 319A-2-1, 111-114 cm and 3-1, 78-81 cm, however, a variety of types are present. The order of crystallization appears to be: large, strongly zoned, equidimensional phenocrysts → small, zoned, square or stubby phenocrysts → lath-shaped phenocrysts → groundmass laths. In addition, 319A-3-1, 78-81 cm contains a

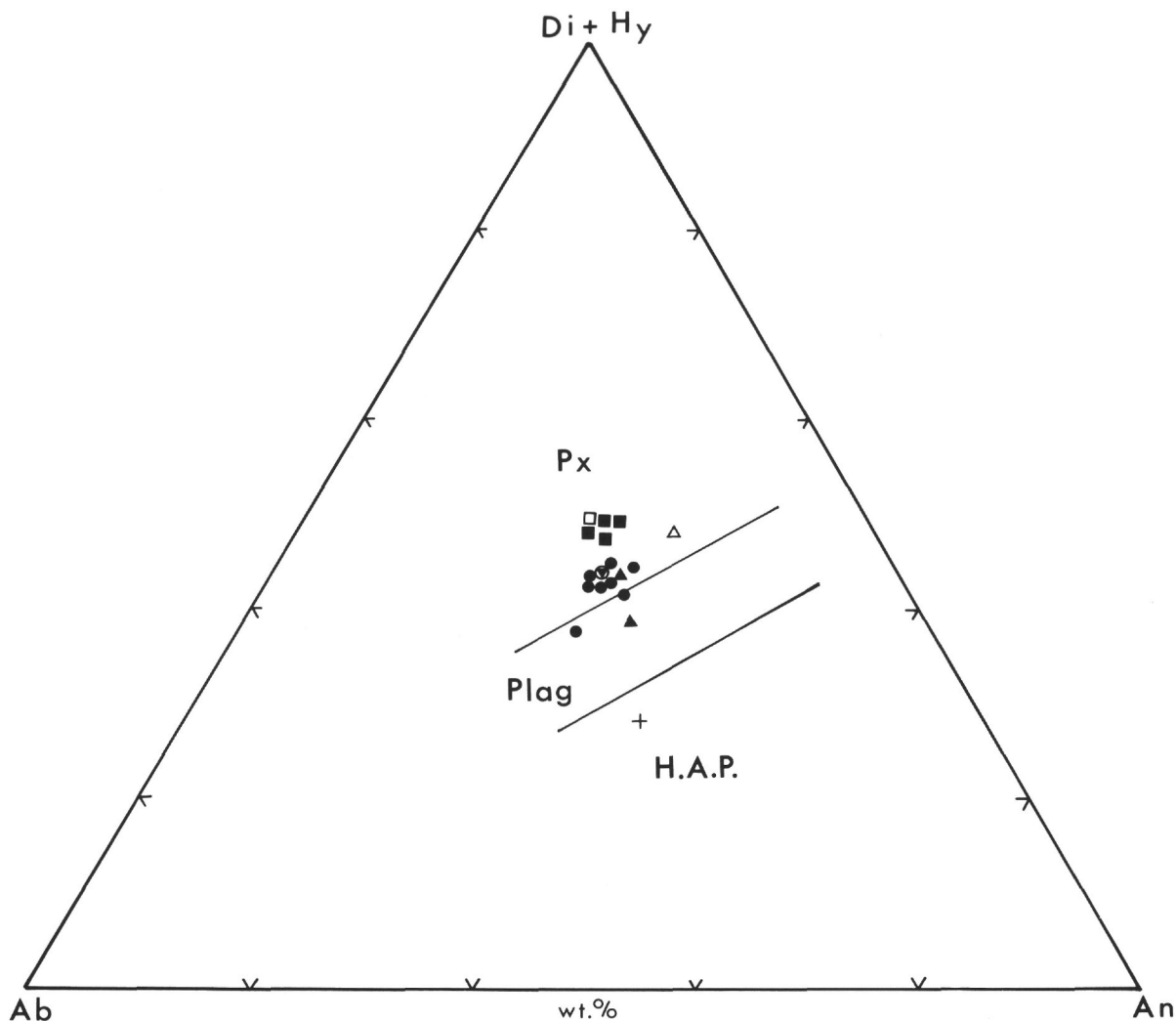


Figure 5. Leg 34 basalts plotted in the normative (normalized) pyroxene, plagioclase, and high-alumina plagioclase tholeiite diagram (di + hy) - ab - an (Hekinian and Aumento, 1973). Symbols as in Figure 4.

single large phenocryst containing a small square plagioclase "inclusion" (An_{61}), which probably represents the core. The large crystal shows reverse zoning, from inner An_{42} to outer rim An_{47} ; the reverse zoning is perhaps produced by pressure fluctuation (Kempe and Schilling, 1974). It is the most sodic feldspar analyzed but only slightly more so than those from 2-1, 111-114 cm.

The FeO^* and MgO contents were determined for some of the phenocrysts. As shown by Bryan (1972) and Bence et al. (1973), FeO^* content is inversely proportional to CaO (Figure 13), and is ascribed to substitution for Al_2O_3 . MgO is low, about 0.2%, although it ranges from 0.1 to 0.3%; as shown by Bence et al., it probably remains virtually constant.

SUMMARY AND CONCLUSIONS

Site 319 Bauer Deep basalt—the longest section—includes porphyritic regions and coarse ophitic rocks with embayed plagioclase. It may represent as many as eight flows or cooling units. Phenocrysts include plagioclase, some small granular pyroxenes, and large

olivines not entirely altered to smectite. The pyroxene is the most calcic augite of the Leg 34 rocks, and the plagioclase lies in the total range An_{42-82} , with at least three types of phenocryst. The olivine could not be determined. The rock is an OL-tholeiite falling in the olivine tholeiite field, but, like all the Leg 34 basalts, is a pyroxene-tholeiite in the classification of Hekinian and Aumento (1973). Again, as with all the Leg 34 basalts, the trace element characterization of Pearce and Cann (1973) shows the rock to be typical OFB. The overall chemistry is typical of LIL-element-depleted MORB; and the basalt is fairly highly fractionated with respect to FeO^*/MgO . Evidence of differentiation is clearly present within the lower part of the 60-meter sequence, showing enrichment upwards in iron and alkalis relative to magnesium and calcium. The upper part, based on two samples, shows a strong trend in the opposite (more "primitive") direction.

Site 320 basalt is variolitic and barely porphyritic, and is thought to occur as thin flows or pillows forming at least 10 cooling units. It is a relatively "primitive" PL-tholeiite, with an average composition falling in the

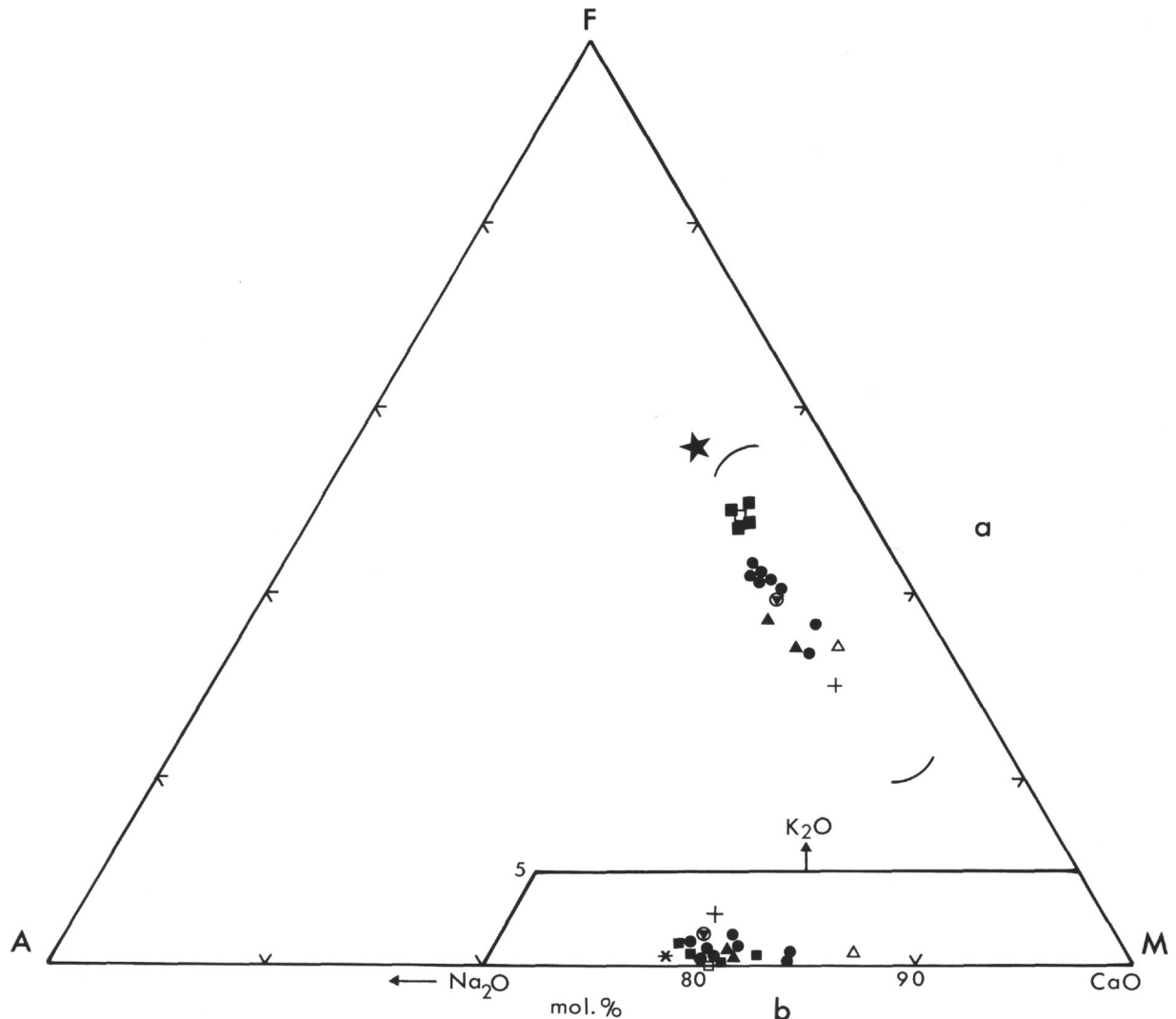


Figure 6. (a) *FMA* diagram of the Leg 34 basalts. Brackets enclose area filled by Mid-Atlantic Ridge rocks, including the iron-rich gabbros, of Miyashiro et al. (1970). Symbols as in Figure 5, with solid star, FETI basalt from Site 32 (Melson, 1973). (b) Lime-alkalis diagram of the Leg 34 basalts. Symbols as in Figure 6a.

quartz tholeiite field, and containing augite and plagioclase near An_{70} .

Site 321 basalt is also from the eastern margin of the Nazca plate. It has a variable texture, with rare phenocrysts, and is fairly vesicular, unlike the first two basalt types. It is thought to represent two extrusive units, although most falls within one unit. Olivine was not noted in the samples studied; the pyroxene is an Al- and Ti-poor augite and the plagioclase An_{60-70} . Again it is a PL-tholeiite, fairly pyroxene-rich, and the most quartz-normative of the Leg 34 rocks. It is highly fractionated and thus of considerable interest. Because of the short cores recovered, differentiation could not be plotted against depth.

However, the Site 320 and 321 basalts are remarkable in that two contrasted types, one relatively "primitive" and one highly fractionated, are found fairly close together, although separated by a fracture zone. A similar situation occurs in the "ancient" crust of the southern Wharton Basin, Southeastern Indian Ocean,

where very "primitive" or primary (?high pressure) basalt (Site 257) occurs fairly close to highly fractionated (?low pressure) FETI-type basalt at Site 256, both showing anomalous differentiation patterns.

ACKNOWLEDGMENTS

Dr. A.C. Bishop is sincerely thanked for reviewing the manuscript and making many helpful suggestions. J.V. Brown took the photomicrographs.

REFERENCES

- Aumento, F. and Loncarevic, B.D., 1969. The Mid-Atlantic Ridge near 45°N. IV. Bald Mountain: Canadian J. Earth Sci., v. 6, p. 11.
- Bass, M.N., Moberly, R.M., Rhodes, J.M., Shih, C-y., and Church, S.E., 1973. Volcanic rocks cored in the central Pacific, Leg 17, Deep Sea Drilling Project. In Winterer, E.L., Ewing, J.I., et al., Initial Reports of the Deep Sea Drilling Project, Volume 17: Washington (U.S. Government Printing Office), p. 429.

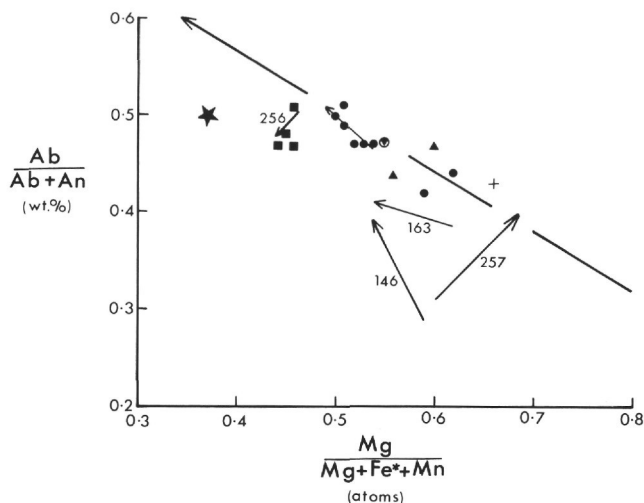


Figure 7. Fractionation diagram ($Ab/[Ab+An]$ vs $Mg/[Mg+Fe^*+Mn]$) for the Leg 34 basalts. Also shown are basalt fractionation trends for Site 163 (Yeats et al., 1973 a, b) and Sites 256 and 257 (Kempe, 1974); the dolerite trend for Site 146 (Donnelly et al., 1973); and the point (solid star) for Site 32 (Melson, 1973). The long broken arrow indicates the generalized fractionation trend for tholeiitic rocks. Symbols as in Figure 6.

Bence, A.E., Papike, J.J., Chandrasekharam, D., Cameron, M., and Camenisch, S., 1973. Petrology of basalts from Leg 15 of the Deep Sea Drilling Project: the central Caribbean: EOS, v. 54, p. 995 (abstract).

Bryan, W.B., 1972. Mineralogical studies of submarine basalts: Yearbook Carnegie Institution Washington, 71, p. 396.

Christensen, N.I., Frey, F.A., MacDougall, D., Melson, W.G., Peterson, M.N.A., Thompson, G., and Watkins, N.D., 1973. Deep Sea Drilling Project: properties of igneous and metamorphic rocks of the oceanic crust: EOS, v. 54, p. 972.

Donnelly, T.W., Melson, W.G., Kay, R., and Rogers, J.J.W., 1973. Basalts and dolerites of Late Cretaceous age from the central Caribbean. In Edgar, N.T., Saunders, J.B., et al., Initial Reports of the Deep Sea Drilling Project, Volume 15: Washington (U.S. Government Printing Office), p. 989.

Engel, A.E.J., Engel, C.G., and Havens, R.G., 1965. Chemical characteristics of oceanic basalts and the upper mantle: Geol. Soc. Am. Bull., v. 76, p. 719.

French, W.J. and Adams, S.J., 1972. A rapid method for the extraction and determination of iron (II) in silicate rocks and minerals: Analyst (London), v. 97, p. 828.

Frey, F.A., Bryan, W.B., and Thompson, G., 1974. Atlantic ocean floor: Geochemistry and petrology of basalts from Legs 2 and 3 of the Deep Sea Drilling Project: J. Geophys. Res., vol. 79, p. 5507.

Hart, S.R., Brooks, C., Krogh, T.E., Davis, G.L., and Nava, D., 1970. Ancient and modern volcanic rocks: a trace element model: Earth Planet. Sci. Lett., v. 10, p. 17.

Hekinian, R., 1971. Chemical and mineralogical differences between abyssal hill basalts and ridge tholeiites in the eastern Pacific Ocean: Marine Geol., v. 11, p. 77.

Hekinian, R. and Aumento, F., 1973. Rocks from the Gibbs fracture zone and the Minia seamount near 53°N in the Atlantic Ocean: Marine Geol., v. 14, p. 47.

Hyndman, R.D., 1974. Seismic velocities of basalts from DSDP Leg 26. In Davies, T.A., Luyendyk, B.P., et al.,

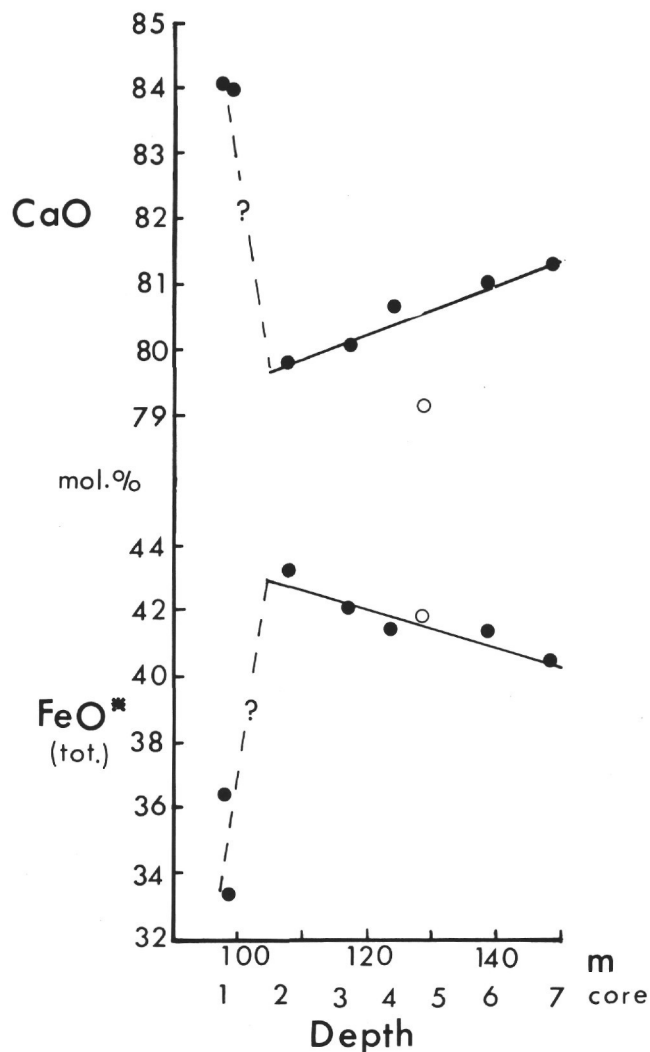


Figure 8. FeO^* from the FMA diagram, and CaO from the lime-alkalis diagram, for Site 319 basalts plotted against depth below the sediment-basalt contact. Open circle, altered material. The linear differentiation may represent fractionation within flows while the more sudden change reflects major differentiation within the magma chamber from which each flow derives.

Initial Reports of the Deep Sea Drilling Project, Volume 26: Washington (U.S. Government Printing Office), p. 509.

Kay, R., Hubbard, N.J., and Gast, P.W., 1970. Chemical characteristics and origin of oceanic ridge volcanic rocks: J. Geophys. Res., v. 75, p. 1585.

Kempe, D.R.C., 1974. The petrology of the basalts, DSDP Leg 26. In Davies T.A., Luyendyk, B.P., et al., Initial Reports of the Deep Sea Drilling Project, Volume 26: Washington (U.S. Government Printing Office), p. 465.

_____, 1975. Normative mineralogy and differentiation patterns of some drilled and dredged oceanic basalts: Contrib. Min. Petrol., v. 50, p. 305.

Kempe, D.R.C. and Schilling, J-G., 1974. Discovery tablemount basalt: petrology and geochemistry: Contrib. Min. Petrol., v. 44, p. 101.

Kuno, H., 1960. High-alumina basalt: J. Petrol., v. 1, p. 121.

Langmyhr, R.J. and Paus, P.E., 1968. The analysis of inorganic siliceous materials by atomic absorption spec-

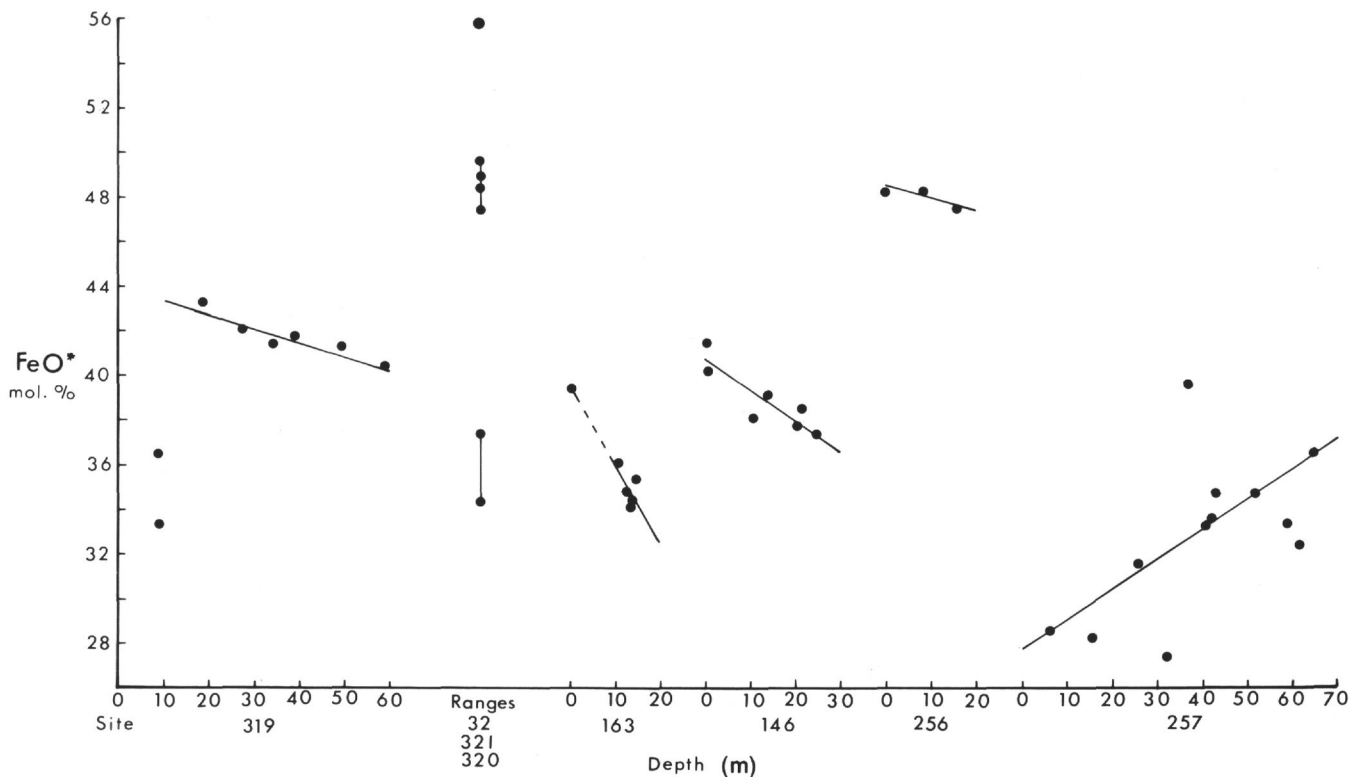


Figure 9. FeO^* from the FMA diagrams plotted against depth below the sediment-basalt contact for all DSDP basalt cores of sufficient length, to show varying fractionation trends. Other values are shown as points or ranges (Sites 32, 320, and 321). Sources of data as in Figure 7.

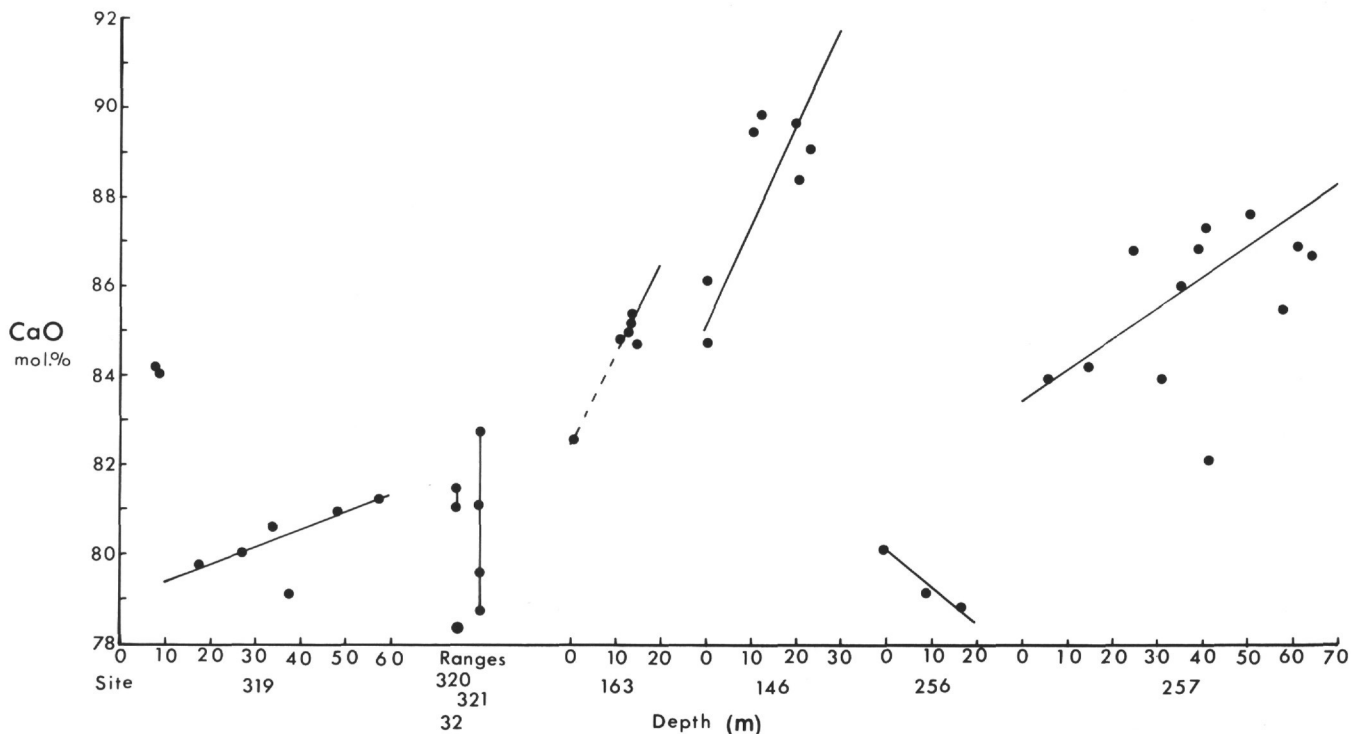


Figure 10. CaO from the lime-alkali diagrams plotted against depth below the sediment-basalt contact for all DSDP basalt cores of sufficient length to show varying fractionation trends. Other values are shown as points or ranges (Sites 32, 320, and 321). Sources of data as in Figure 7.

TABLE 7
Pyroxene Analyses, Site 319A^a

	2-1, 111-114 cm			3-1, 78-81 cm				5-1, 20-22 cm	7-1, 121-124 cm		
	Phenocryst (av. of 2)	Plumose "Crystals" (av. of 2)	Mosaic Groundmass	Phenocryst Core	Phenocryst Rim	Phenocryst (Core)	Phenocryst (Near Core)	Groundmass (av. of 3)	Groundmass (av. of 4)	Groundmass	Groundmass (av. of 2)
SiO ₂	49.22	49.18	49.39	50.93	50.44	51.06	50.48	50.68	49.92	49.13	49.61
TiO ₂	1.55	1.68	1.75	1.12	1.24	1.12	1.26	1.39	1.59	1.65	1.83
Al ₂ O ₃	5.20	4.32	5.77	3.45	2.24	2.98	2.55	3.72	4.11	4.40	3.86
Cr ₂ O ₃	n.d. ^b	n.d. ^b	n.d. ^b	0.26	nil	0.12	nil	0.19	0.13	n.d. ^b	n.d. ^b
FeO*	9.89	11.01	8.11	8.27	13.23	10.16	13.08	8.67	8.66	10.80	12.35
MnO	0.20	0.24	0.13	0.24	0.36	0.28	0.33	0.23	0.23	n.d. ^b	n.d. ^b
MgO	14.04	13.99	14.53	15.66	14.13	15.39	14.28	15.85	15.30	13.94	13.50
CaO	19.53	19.80	20.41	20.00	18.13	19.06	18.47	19.49	19.64	19.58	18.68
Na ₂ O	0.32	0.34	0.28	0.32	0.32	0.31	0.30	0.30	0.35	0.35	0.35
K ₂ O	n.d. ^b	n.d. ^b	n.d. ^b	n.d. ^b	n.d. ^b	n.d. ^b	n.d. ^b	n.d. ^b	0.02	n.d. ^b	n.d. ^b
Total	99.95	100.56	100.37	100.25	100.09	100.48	100.75	100.52	99.95	99.85	100.18
Mg	42.0	40.7	43.1	45.2	40.9	44.2	40.9	45.7	44.5	40.9	39.9
Fe	16.2	18.0	13.5	13.4	21.5	16.4	21.0	14.0	14.3	17.8	20.5
Ca	41.8	41.3	43.4	41.4	37.6	39.4	38.1	40.3	41.2	41.3	39.6

^aAnalysts: R.F. Symes and J.C. Bevan (by electron microprobe).

^bn.d. = not determined.

TABLE 8
Pyroxene Analyses, Hole 320B and Site 321^a

	320B-3-1, 54-57 Groundmass (av. of 2)	320B-3-1, 54-57 Groundmass	321-14-4, 7-10 Groundmass (av. of 2)	321-14-4, 7-10 Groundmass (av. of 2)	321-14-4, 7-10 Groundmass
SiO ₂	49.51	50.88	51.32	51.52	50.63
TiO ₂	1.57	1.94	0.93	1.05	1.13
Al ₂ O ₃	5.07	5.73	2.46	2.81	2.65
Cr ₂ O ₃	n.d. ^b	n.d. ^b	n.d. ^b	n.d. ^b	n.d. ^b
FeO*	7.95	10.95	9.69	11.24	12.32
MnO	n.d. ^b	n.d. ^b	0.08	n.d. ^b	0.25
MgO	16.30	15.72	16.71	16.00	15.40
CaO	18.90	14.46	17.93	18.34	17.56
Na ₂ O	0.25	0.33	0.13	0.09	0.20
K ₂ O	n.d. ^b	n.d. ^b	0.02	0.03	0.06
Total	99.55	100.01	99.27	101.08	100.20
Mg	47.4	48.7	47.7	45.1	44.1
Fe	13.1	19.1	15.5	17.8	19.8
Ca	39.5	32.2	36.8	37.1	36.1

^aAnalysts: R.F. Symes and J.C. Bevan (by electron microprobe).

^bn.d. = not determined.

trophotometry and the hydrofluoric acid decomposition technique. Part I: the analysis of silicate rocks: *Anal. Chim. Acta*, v. 43, p. 397.

Mason, P.K., Frost, M.T., and Reed, S.J.B., 1969. B.M.-I.C.-N.P.L. computer program for calculating corrections in quantitative X-ray microanalysis: *Nat. Phys. Lab. (U.K.) Rept. 1*.

Melson, W.G., 1973. Basaltic glasses from the Deep Sea Drilling Project: chemical characteristics, compositions of alteration products, and fission track 'ages': *EOS*, v. 54, p. 1011 (abstract).

Norrish, K. and Hutton, J.T., 1969. An accurate X-ray spectrographic method for the analysis of a wide range of geological samples: *Geochim. Cosmochim. Acta*, v. 33, p. 431.

Pearce, J.A. and Cann, J.R., 1973. Tectonic setting of basic volcanic rocks determined using trace element analyses: *Earth Planet. Sci. Lett.*, v. 19, p. 290.

Shido, F., Miyashiro, A., and Ewing, M., 1971. Crystallization of abyssal tholeiites: *Contrib. Min. Petrol.*, v. 31, p. 251.

Sweatman, T.R. and Long, J.V.P., 1969. Quantitative electron-probe microanalysis of rock-forming minerals: *J. Petrol.*, v. 10, p. 332.

TABLE 9
Plagioclase Feldspar Analyses, Sample 319A-2-1, 111-114 cm^a

	Zoned Square Phenocryst		Large Square Phenocryst	Untwinned Irregular Phenocryst	Lath-Type Phenocryst		Groundmass (av. of 3)
	Core	Rim			Core (av. of 2)	Rim	
SiO ₂	48.08	52.91	50.12	52.43	51.04	55.51	56.59
Al ₂ O ₃	32.24	28.26	31.17	29.14	29.08	26.64	26.84
FeO*	0.47	n.d. ^b	0.52	0.72	0.74	n.d. ^b	n.d. ^b
MgO	n.d. ^b	n.d. ^b	n.d. ^b	n.d. ^b	n.d. ^b	n.d. ^b	n.d. ^b
CaO	16.24	12.63	14.76	13.08	13.79	9.92	9.83
Na ₂ O	2.44	4.55	3.17	4.25	4.03	6.28	5.88
K ₂ O	0.04	0.05	0.04	0.05	0.06	0.09	0.08
Total	99.51	98.40	99.78	99.67	98.74	98.44	99.22
Ab	21.3	39.3	27.9	36.9	34.5	53.1	51.7
An	78.5	60.4	71.8	62.8	65.2	46.4	47.8
Or	0.2	0.3	0.2	0.3	0.3	0.5	0.5

^aAnalysts: R.F. Symes and J.C. Bevan (by electron microprobe).

^bn.d. = not determined.

TABLE 10
Plagioclase Feldspar Analyses, Sample 319A-3-1, 78-81 cm^a

Phenocryst	Lath-Type Phenocryst		Lath-Type Phenocryst		Small Square Phenocryst		Large Phenocryst With Square Inclusion			Groundmass			
	Core	Rim	Core	Rim	Core (av. of 2)	Rim	Core	Rim	Inclusion	(av. of 2)	Groundmass		
SiO ₂	48.26	54.49	48.63	52.90	52.92	56.81	53.61	54.37	58.84	57.92	53.99	53.29	54.02
Al ₂ O ₃	32.76	28.26	31.99	29.98	29.40	26.77	29.09	28.46	25.29	26.19	28.18	29.17	27.79
FeO*	0.40	n.d. ^b	0.52	n.d. ^b	0.71	n.d. ^b	0.71	n.d. ^b	0.78	n.d. ^b	n.d. ^b	n.d. ^b	n.d. ^b
MgO	0.20	n.d. ^b	0.17	n.d. ^b	0.23	n.d. ^b	0.24	n.d. ^b	0.11	n.d. ^b	n.d. ^b	n.d. ^b	n.d. ^b
CaO	17.12	11.89	16.61	13.41	13.32	9.86	12.90	12.32	8.79	9.53	12.70	12.66	11.83
Na ₂ O	2.10	4.74	2.21	3.86	4.18	5.80	4.30	4.89	6.72	5.97	4.49	4.20	5.15
K ₂ O	0.03	0.06	0.03	0.06	0.06	0.08	0.05	0.06	0.11	0.10	0.05	0.05	0.06
Total	100.87	99.44	100.16	100.21	100.82	99.32	100.90	100.10	100.64	99.71	99.41	99.37	98.85
Ab	18.0	41.8	19.2	34.2	36.0	51.3	37.6	41.7	57.3	52.5	38.7	37.3	43.8
An	81.8	57.7	80.6	65.3	63.5	48.2	61.9	57.8	41.9	46.7	60.8	62.2	55.8
Or	0.2	0.5	0.2	0.5	0.5	0.5	0.5	0.5	0.8	0.8	0.5	0.5	0.4

^aAnalysts: R.F. Symes and J.C. Bevan (by electron microprobe).

^bn.d. = not determined.

Yeats, R.S., Forbes, W.C., Heath, G.R., and Scheidegger, K.F., 1973a. Petrology and geochemistry of DSDP Leg 16 basalts, eastern equatorial Pacific. *In* van Andel, T.H., Heath, G.R., et al., Initial Reports of the Deep Sea Drilling Project, Volume 16: Washington (U.S. Government Printing Office), p. 617.

Miyashiro, A., Shido, F., and Ewing, M., 1969. Diversity and origin of abyssal tholeiite from the Mid-Atlantic Ridge near 24° and 30° North latitude: *Contrib. Min. Petrol.*, v. 23, p. 38.

_____, 1970. Crystallization and differentiation in abyssal tholeiites and gabbros from mid-oceanic ridges: *Earth Planet. Sci. Lett.*, v. 7, p. 361.

Yeats, R.S., Forbes, W.C., Scheidegger, K.F., Heath, G.R., and van Andel, T.J.H., 1973b. Core from Cretaceous basalt, central equatorial Pacific, Leg 16, Deep Sea Drilling Project: *Geol. Soc. Am. Bull.*, v. 84, p. 871.

Yoder, H.S., Jr., and Tilley, C.E., 1962. Origin of basalt magmas: an experimental study of natural and synthetic rock systems: *J. Petrol.*, v. 3, p. 342.

TABLE 11
Plagioclase Feldspar Analyses, Sample 319A-5-1, 20-22 cm^a

	Zoned Euhedral Phenocryst (Core)	Lath-Type Phenocryst (Core)	Lath-Type Phenocryst	Stubby Phenocryst	Groundmass (av. of 2)
SiO ₂	48.12	48.57	49.24	52.43	52.88
Al ₂ O ₃	31.33	31.49	30.64	27.93	28.52
FeO*	0.48	0.41	0.50	0.72	n.d. ^b
MgO	0.20	0.24	0.21	0.27	n.d. ^b
CaO	17.00	16.58	16.06	13.65	13.01
Na ₂ O	2.16	2.41	2.54	3.62	4.09
K ₂ O	0.02	0.04	0.04	0.05	0.05
Total	99.31	99.74	99.23	98.67	98.55
<i>Ab</i>	18.7	20.8	22.2	32.3	36.1
<i>An</i>	81.2	79.0	77.5	67.4	63.6
<i>Or</i>	0.1	0.2	0.2	0.3	0.3

^aAnalysts: R.F. Symes and J.C. Bevan (by electron microprobe).

^bn.d. = not determined.

TABLE 12
Plagioclase Feldspar Analyses, Sample 319A-7-1, 121-124 cm^a

	Phenocryst	Groundmass	Groundmass (av. of 3)
SiO ₂	51.76	49.49	52.16
Al ₂ O ₃	30.09	31.50	28.81
FeO*	0.60	n.d. ^b	n.d. ^b
MgO	0.25	n.d. ^b	n.d. ^b
CaO	14.11	15.71	13.52
Na ₂ O	3.58	2.20	3.78
K ₂ O	0.05	0.02	0.06
Total	100.44	98.92	98.33
<i>Ab</i>	31.4	20.2	33.5
<i>An</i>	68.3	79.7	66.2
<i>Or</i>	0.3	0.1	0.3

^aAnalysts: R.F. Symes and J.C. Bevan (by electron microprobe).

^bn.d. = not determined.

TABLE 13
Plagioclase Feldspar Analyses, Sample 320B-3-1, 54-57 cm^a

	Phenocryst		Small Phenocryst		Groundmass (av. of 2)
	Core	Rim	Core (av. of 4)	Rim	
SiO ₂	50.91	52.17	51.72	53.86	51.81
Al ₂ O ₃	31.08	29.86	30.06	27.82	29.99
FeO*	0.52	n.d. ^b	0.62	n.d. ^b	n.d. ^b
MgO	n.d. ^b	n.d. ^b	n.d. ^b	n.d. ^b	n.d. ^b
CaO	15.49	14.36	14.48	13.09	14.43
Na ₂ O	3.17	3.69	3.50	4.11	3.47
K ₂ O	0.05	0.06	0.05	0.06	0.05
Total	101.22	100.14	100.43	98.94	99.75
<i>Ab</i>	27.0	31.6	30.3	36.1	30.2
<i>An</i>	72.7	68.0	69.4	63.6	69.5
<i>Or</i>	0.3	0.3	0.3	0.3	0.3

^aAnalysts: R.F. Symes and J.C. Bevan (by electron microprobe).
^bn.d. = not determined.

TABLE 14
Plagioclase Feldspar Analyses, Sample 321-14-4, 7-10 cm^a

	Phenocryst		Phenocryst		Groundmass
	Core (av. of 2)	Rim (av. of 2)	Core (av. of 3)	Rim	
SiO ₂	51.76	52.59	52.88	53.49	52.75
Al ₂ O ₃	29.15	29.08	28.16	27.69	28.87
FeO*	0.74	n.d. ^b	0.72	n.d. ^b	n.d. ^b
MgO	0.16	n.d. ^b	0.20	n.d. ^b	n.d. ^b
CaO	14.25	12.95	13.14	11.89	12.63
Na ₂ O	3.48	3.96	4.06	4.95	4.48
K ₂ O	0.07	0.07	0.07	0.06	0.07
Total	99.61	98.65	99.23	98.08	98.80
<i>Ab</i>	30.6	35.5	35.7	42.8	39.0
<i>An</i>	69.0	64.1	63.9	56.9	60.6
<i>Or</i>	0.4	0.4	0.4	0.3	0.4

^aAnalysts: R.F. Symes and J.C. Bevan (by electron microprobe).
^bn.d. = not determined.

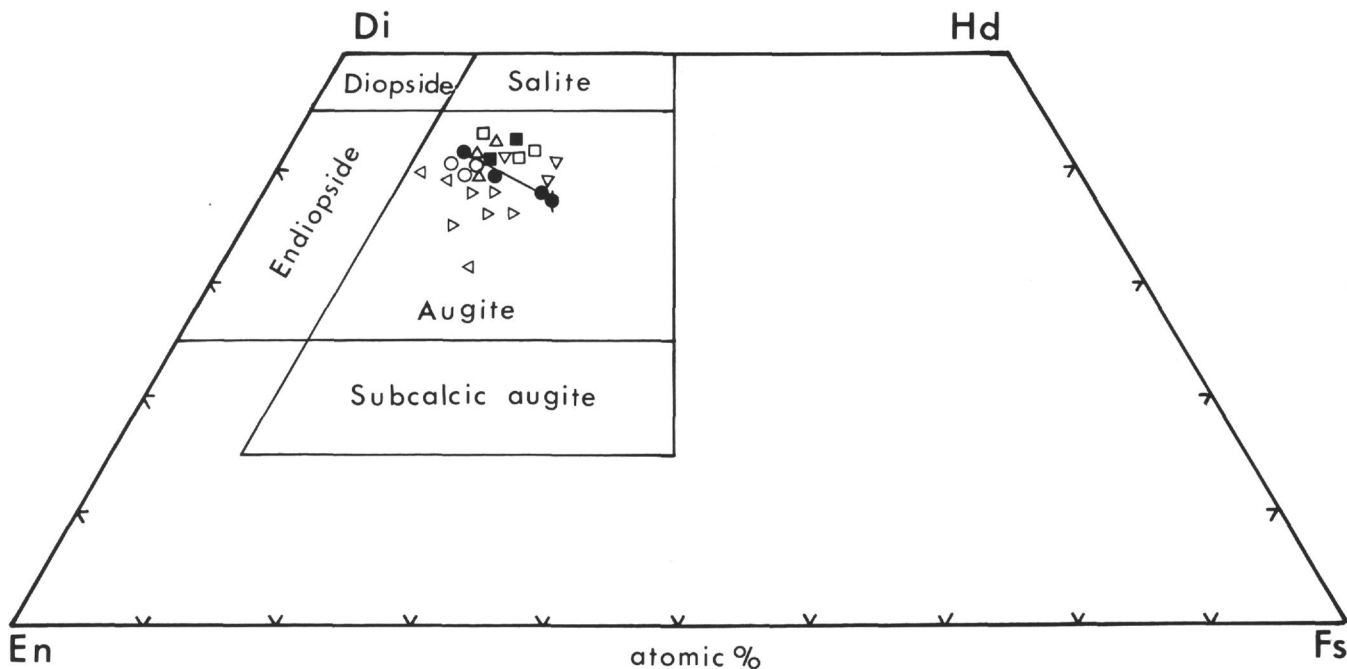


Figure 11. Pyroxene compositions from the Leg 34 basalts from Sites 319, 320, and 321. ■ □ 319A-2-1; ● ○ 319A-3-1; △ 319A-5-1; ▽ 319A-7-1; ◁ 320B-3-1; △ 321-14-4; Solid symbols, phenocryst, or phenocryst core ♦ phenocryst rim, joined to core with tie line; Open symbols, groundmass.

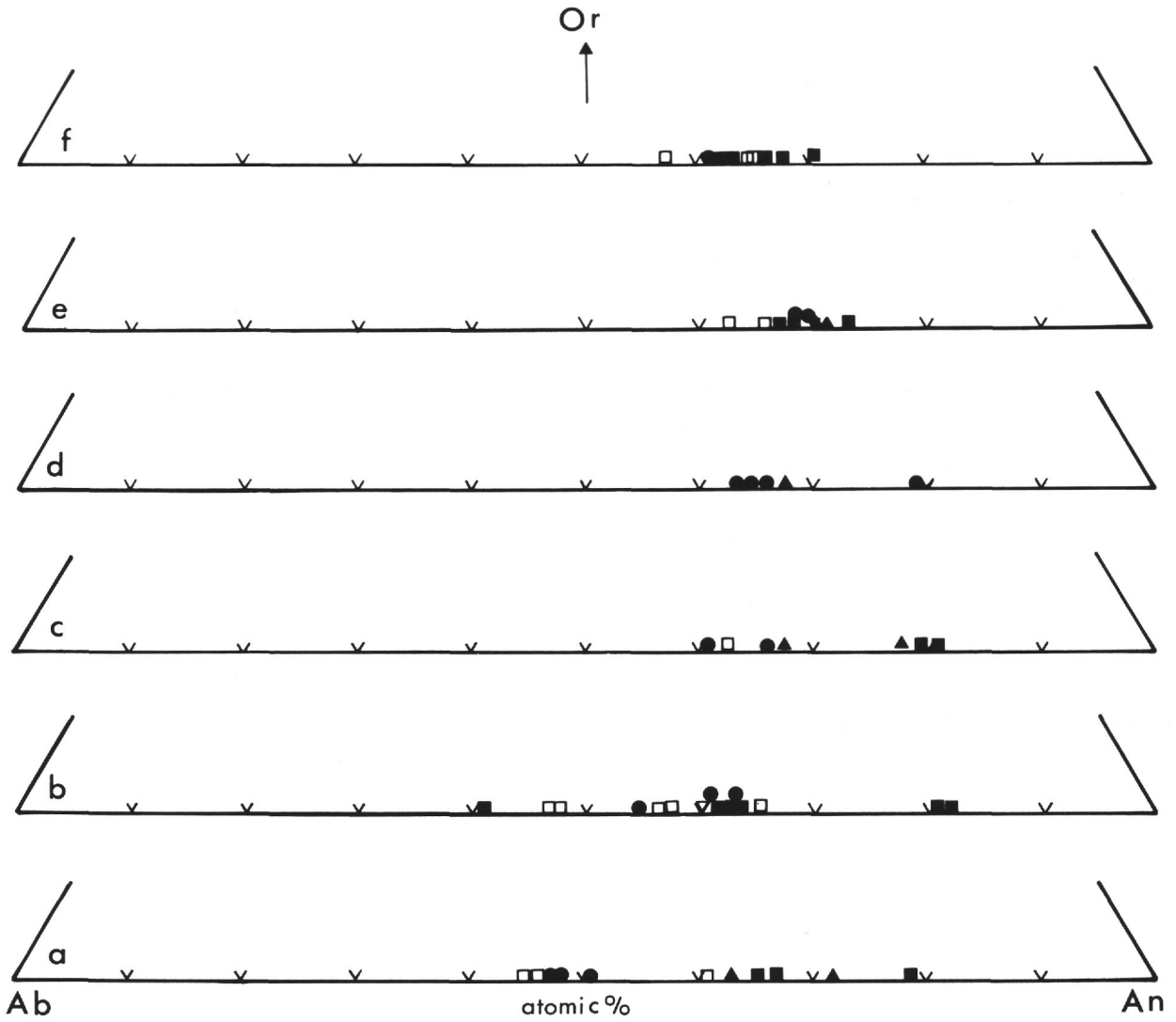


Figure 12. Plagioclase feldspar compositions from the Leg 34 basalts from (a) 319A-2-1; (b) 319A-3-1; (c) 319A-5-1; (d) 319A-7-1; (e) 320B-3-1; and (f) 321-14-4. ■ phenocryst core; □ phenocryst rim; ▲ phenocryst; ● groundmass lath; “inclusion” in phenocryst from 319A-3-1; □ in (c) represents the least calcic limit of zoning and not a precise analysis.

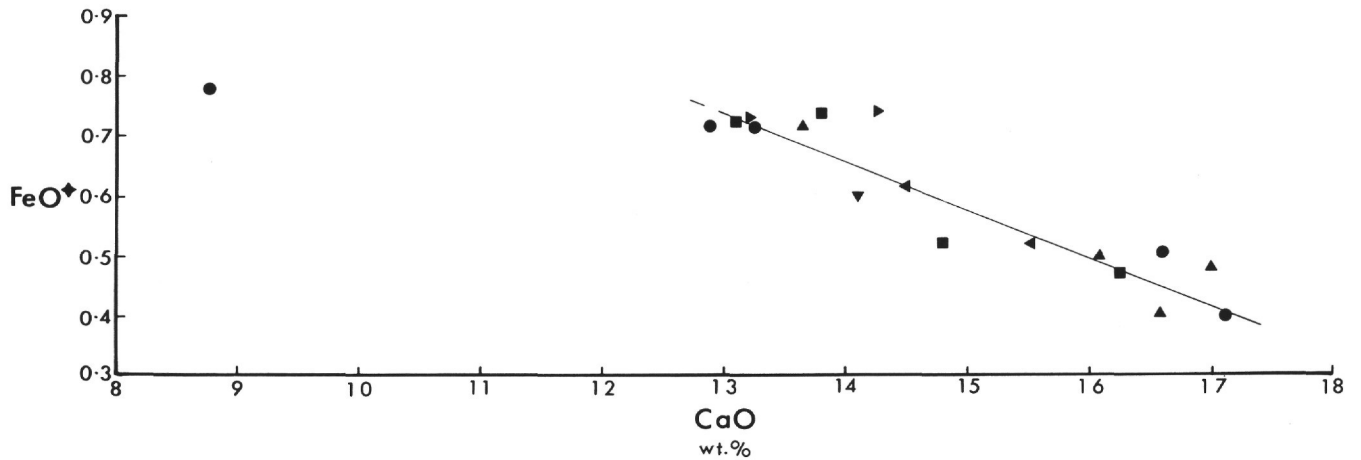
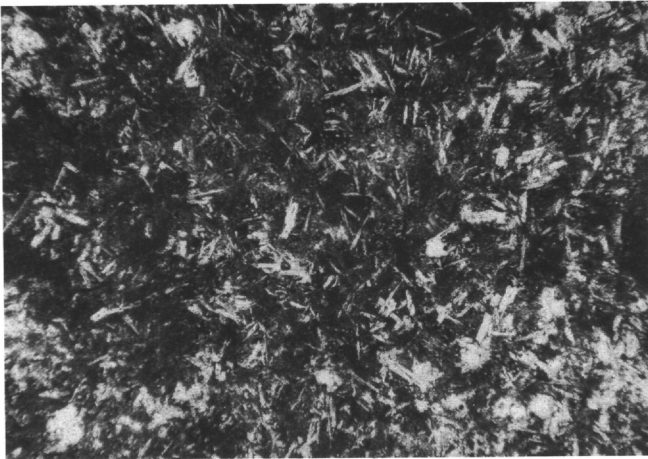


Figure 13. FeO* plotted against CaO (wt%) in plagioclase phenocrysts from Site 319A: ■ 319A-2-1, ● 319A-3-1, ▲ 319A-5-1, ▼ 319A-7-1, ◀ 320B-3-1; ▲ 321-14-4.

PLATE 1

- Figure 1 Photomicrograph of variolitic basalt, Bauer Deep (319-13-1, 77-80 cm). Plane polarized light (ppl), $\times 14$.
- Figure 2 Photomicrograph of coarse variolitic basalt (319A-2-1, 111-114 cm). Note zoned plagioclase phenocryst and large pyroxene grains. This rock contains a few grains of celadonite. Crossed polars, $\times 14$.
- Figure 3 Photomicrograph of ophitic basalt (319A-3-1, 78-81 cm). Note embayed plagioclase laths, apparently formed around preexisting pyroxene, and "runic" texture within the sheaves of pyroxene crystals. Ppl, $\times 14$.
- Figure 4 Photomicrograph of subophitic basalt, with some phenocrysts (319A-3-5, 75-78 cm). Note small phenocrysts of olivine completely altered to smectite. Crossed polars, $\times 14$.
- Figure 5 Photomicrograph of porphyritic, hyaloophitic basalt (319A-5-1, 20-22 cm). Note plagioclase phenocrysts, altered olivine, and glassy "pools." Crossed polars, $\times 14$.
- Figure 6 Photomicrograph of glassy basalt (319A-6-1, 93-98 cm). This rock contains very small fresh olivines. Ppl, $\times 14$.

PLATE 1



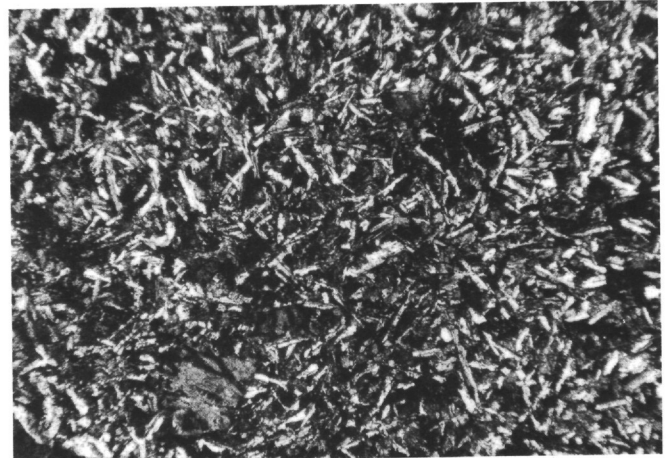
1



2



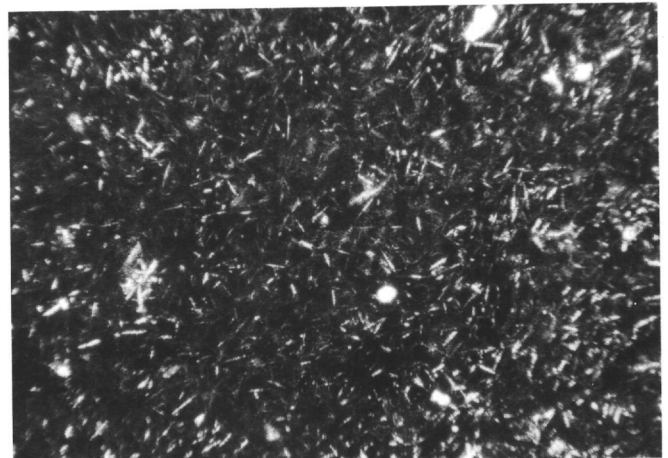
3



4



5

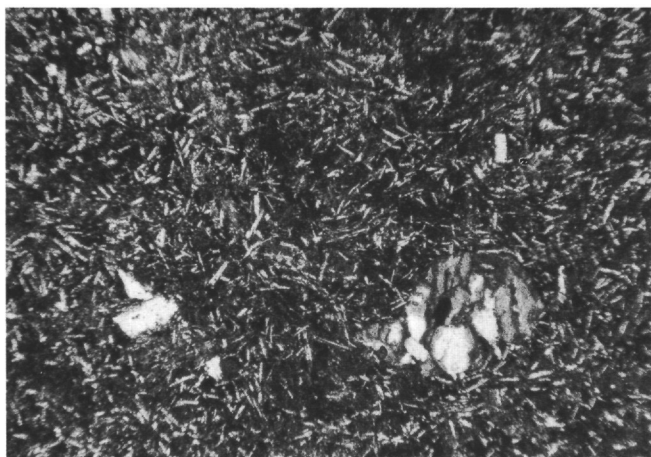


6

PLATE 2

- Figure 1 Photomicrograph of porphyritic subvariolithic basalt (319A-7-1, 121-124 cm). Note large (2 mm) phenocryst of olivine, not entirely altered to smectite, and small plagioclase phenocryst. Ppl, $\times 14$.
- Figure 2 Photomicrograph of porphyritic variolithic basalt from the eastern margin of the Nazca plate (320B-3-1, 54-57 cm). Note small phenocrysts and bifurcate microlites of plagioclase. Ppl, $\times 14$.
- Figure 3 Photomicrograph of variolithic basalt (320B-5, CC). Note plumose or feathery pyroxene microlites. Ppl, $\times 14$.
- Figure 4 Photomicrograph of vesicular hyaloophitic basalt (321-14-1, 42-45 cm). Most of the vesicles are empty. The texture in the "islands" is fine grained subophitic, with many embayed plagioclase crystals. Ppl, $\times 14$.
- Figure 5 Photomicrograph of vesicular hyaloophitic basalt (321-14-2, 9-12 cm). The vesicles are filled with calcite. Ppl, $\times 14$.
- Figure 6 Photomicrograph of coarse hyaloophitic, subophitic basalt (321-14-4, 7-10 cm). Note microphenocrystic laths of plagioclase and embayed feldspar grains clustered with pyroxene. Crossed polars, $\times 14$.

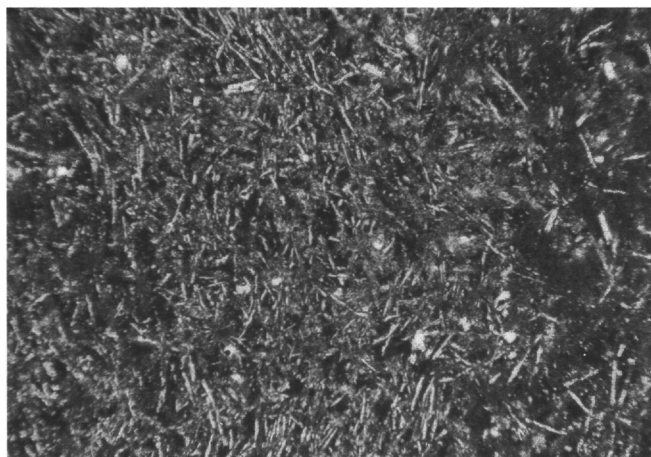
PLATE 2



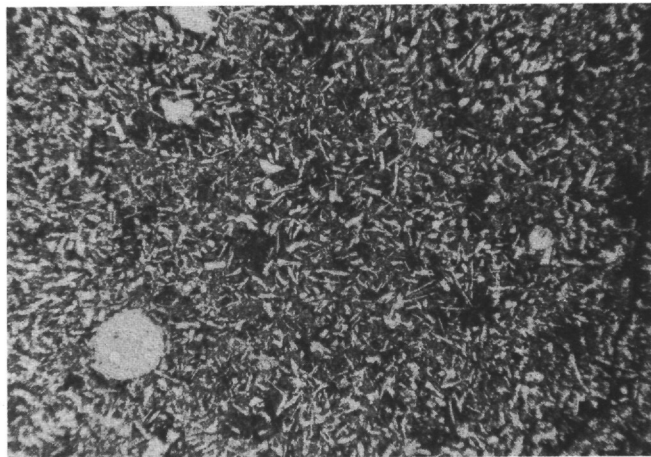
1



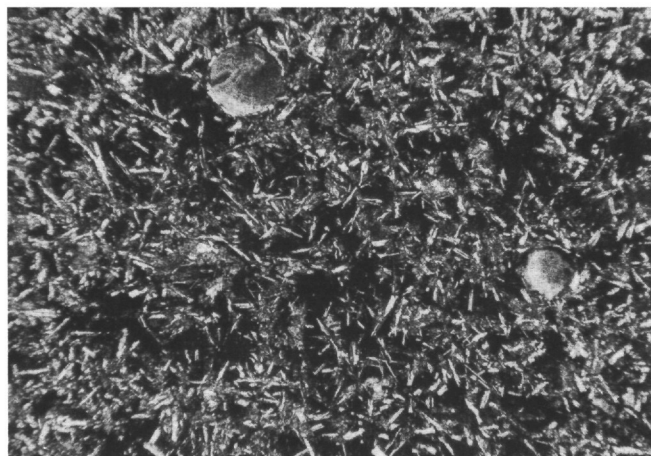
2



3



4



5



6